

Recent Advances in Dendritic Macromonomers for Hydrogel Formation and Their Medical Applications

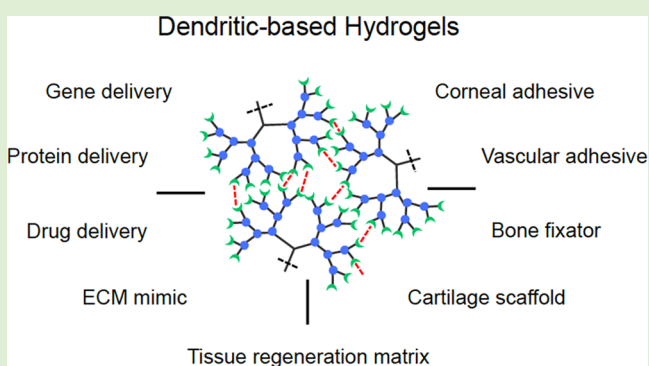
Cynthia Ghobril,[†] Edward K. Rodriguez,[‡] Ara Nazarian,[§] and Mark W. Grinstaff^{*,†}

[†]Departments of Biomedical Engineering, Chemistry and Medicine, Boston University, 590 Commonwealth Avenue, Boston, Massachusetts 02215, United States

[‡]Carl J. Shapiro Department of Orthopaedic Surgery, Beth Israel Deaconess Medical Center, Harvard Medical School, Boston, Massachusetts, United States

[§]Center for Advanced Orthopaedic Studies, Carl J. Shapiro Department of Orthopaedic Surgery, Beth Israel Deaconess Medical Center, Harvard Medical School, Boston, Massachusetts, United States

ABSTRACT: Hydrogels represent one of the most important classes of biomaterials and are of interest for various medical applications including wound repair, tissue engineering, and drug release. Hydrogels possess tunable mechanical properties, biocompatibility, nontoxicity, and similarity to natural soft tissues. The need for hydrogels with specific properties, based on the design requirements of the *in vitro*, *in vivo*, or clinical application, motivates researchers to develop new synthetic approaches and cross-linking methodologies to form novel hydrogels with unique properties. The use of dendritic macromonomers represents one elegant strategy for the formation of hydrogels with specific properties. Specifically, the uniformity of dendrimers combined with the control of their size, architecture, density, and surface groups make them promising cross-linkers for hydrogel formation. Over the last two decades, a large variety of dendritic-based hydrogels are reported for their potential use in the clinic. This review describes the state of the art with these different dendritic hydrogel formulations including their design requirements, the synthetic routes, the measurement and determination of their properties, the evaluation of their *in vitro* and *in vivo* performances, and future perspectives.



1. INTRODUCTION

The report by Wichterle and Lim in 1960 entitled “Hydrophilic Gels for Biological Use”, initiated a new field of research, and today, hydrophilic gels or hydrogels are actively studied.¹ Hydrogels are three-dimensional (3D) water-swelling cross-linked networks, which are composed of small molecules or macromolecules connected together by multiple physical and/or covalent bonds.^{2–4} These materials retain large amounts of water (up to 99%) due to the presence of hydrophilic moieties such as amino, hydroxyl, ether or carboxylic groups, in their backbones or side chain structures. Hydrogels can be prepared from biocompatible and biodegradable precursors, including those that are naturally occurring (e.g., glycerol).⁵ Their high water content, porous, and 3D matrix are ideal for the encapsulation of small molecules and proteins as well as cells. Importantly, the composition, structure, and cross-linking chemistry can be tuned to exhibit the desired mechanical properties or degradation rate for a specific *in vitro*, *in vivo*, or clinical application. Consequently, hydrogels are widely used in various biomedical applications such as tissue engineering, drug delivery, wound repair, cell encapsulation, and bioimaging.^{6–15} Dendrimer, PEG star, hyperbranched, and linear polymers are used as macromonomers for hydrogel formation. The PEG star

and hyperbranched polymers are often used over dendrimers, due to these polymers being more easily synthesized. These hydrogels will not be discussed, and the reader is referred to several recent articles, which highlight the utility of PEG star and hyperbranched polymers for hydrogel preparation.^{16–24} Recently, hydrogels composed of dendritic macromonomers have garnered interest in the biomedical field. Dendrimers are uniform branched macromolecules composed of a focal point/core, repeating branching units (generations, G), and multiple peripheral functional groups. These macromonomers can be synthesized with defined sizes, architectures, and reactive end groups, and are subsequently used to prepare dendritic-based hydrogels with interesting features, modes of action, and physicochemical properties.^{25–30} Specifically, when dendritic G_n macromolecules composed of multiple functional groups react together or with other multiple functional molecules/polymers, water-swelling 3D cross-linked networks (i.e., hydrogels) are formed.^{31,32} The compositional preciseness and known architecture of dendrimers enables the development

Received: January 3, 2016

Revised: March 7, 2016

Published: March 15, 2016

of well-defined composition–structure–property relationships, which facilitate further research and fabrication of optimized hydrogels with specific properties. In addition, the high degree of functionality of the dendrimer allows formation of hydrogel cross-links as well as introduction of additional chemical reactive groups for advanced functions (e.g., drug delivery). Development of such relationships can be more limiting or challenging with hyperbranched, star, or linear polymers. However, recent advances in polymer synthesis have afforded these macromolecules with better control of molecular weight and composition. Over the last two decades, various dendritic-based hydrogels are described for biomedical applications. This review begins with a discussion of the synthesis and properties of dendritic hydrogels, followed by an evaluation of their uses in wound repair, tissue engineering, and drug and gene delivery, and concludes with a summary and future directions.

2. PREPARATION AND PROPERTIES OF DENDRITIC HYDROGELS

Dendritic hydrogels are commonly synthesized by physical or chemical gelation, as depicted in Figure 1. Dendritic macro-

Dendrimers/dendrons

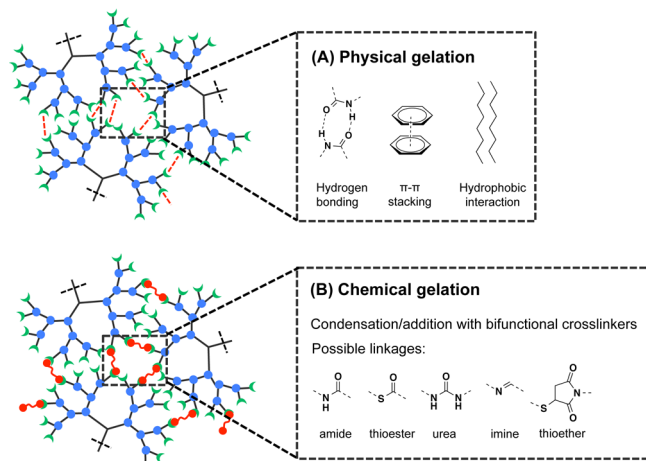


Figure 1. Examples of dendritic hydrogel formation through (A) physical and (B) chemical gelation.

monomers possessing functionalized groups can cross-link by physical or chemical interactions with other similarly or complementarily functionalized macromonomers to form water-swappable 3D networks known as hydrogels. The dendritic structure, focal point, and number of end groups can be easily tuned for the preparation of hydrogels with controlled features and enhanced properties, making these macromonomers ideal for the design of such materials. The following section describes the reported physical and chemical linkages for the preparation of these materials. Moreover, the selection of the specific cross-linking chemistry significantly influences the material properties of these biomaterials.

2.1. Physical Gelation. Physical dendritic hydrogels are formed when dendritic macromolecules cross-link with each other and form water-swappable 3D networks through reversible interactions such as hydrogen bonding, ionic association, molecular entanglement (i.e., with dendritic hybrids), hydrophobic interaction, host–guest complexation, and metal coordination (i.e., physical gelation; Figure 1A). Physical gelation generates stimuli-responsive dendritic hydrogels that

are often used, for example, for controlled-release type applications due to the noncovalent linkages in the network that tend to disrupt in response to stress or physical changes (i.e., pH, ionic strength, temperature) in the body.

In 1990, Newkome and co-workers described the first example of physical dendritic hydrogels formed by the cross-linking of dendritic macromolecules via intermolecular hydrogen bonding and hydrophobic interactions.³³ The macromonomers were composed of two branched domains with hydroxyl end groups connected through a lipophilic spacer of variable lengths (Figure 2). The dendrimers formed thermor-

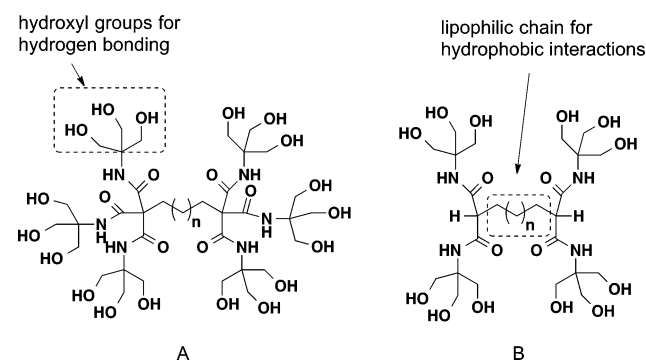
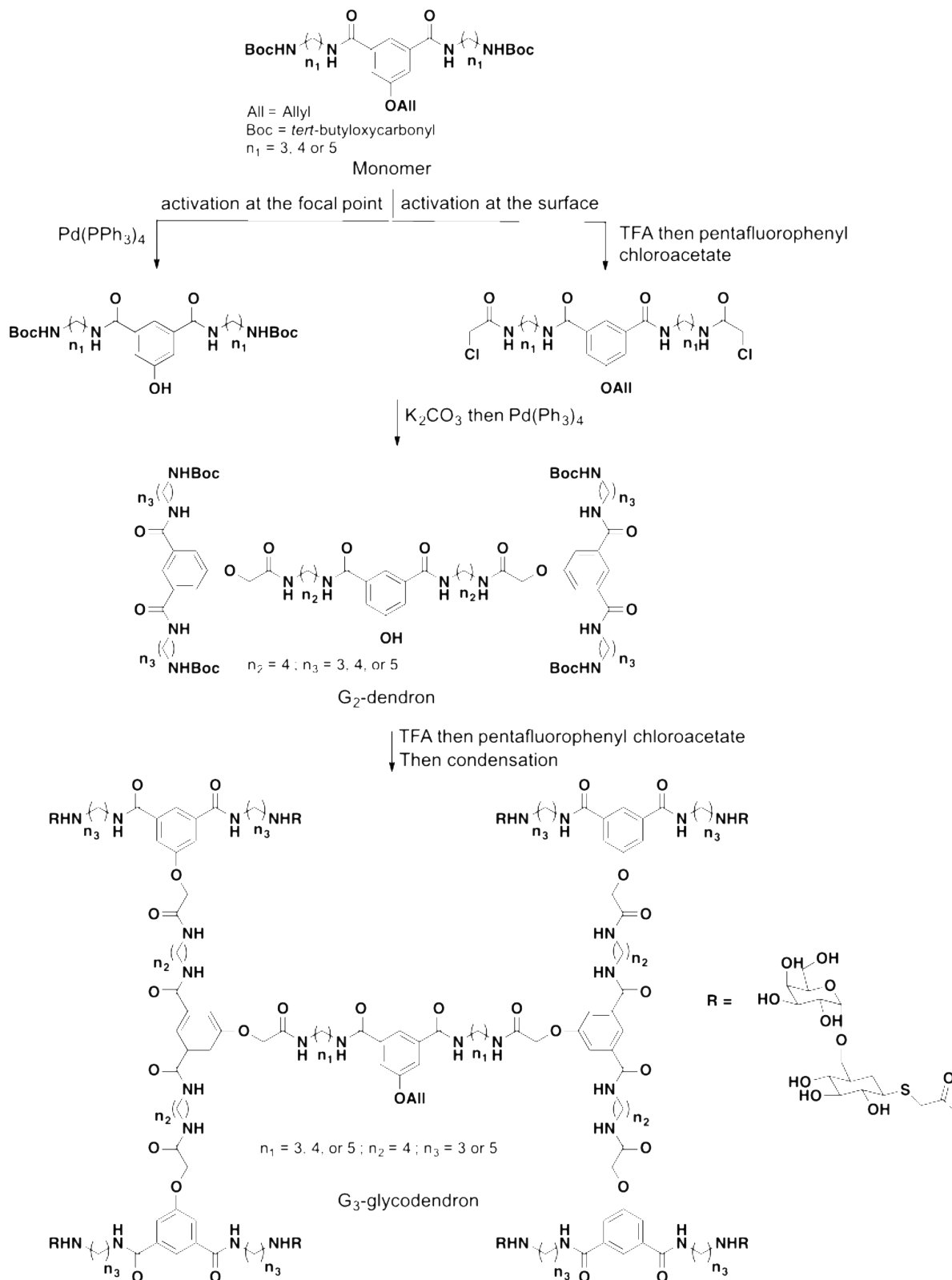


Figure 2. Structures of A and B macromonomers developed by Newkome and co-workers.³³

versible hydrogels at concentrations as low as one weight percentage (wt %) after heating the aqueous solution to 80 °C then cooling it to 25 °C. The gelation properties were determined by viscometry, optical and electronic microscopy, and light scattering. For example, aqueous solutions of arborol A ($n = 8$) exhibited different phase transition temperatures depending on the concentration of the dendrimer in the solution, with higher dendritic concentrations (8.15 wt %) exhibiting higher gel to solution temperatures (69–70 °C). Both arborols A and B ($n = 8$) formed stable gels in the pH range of 2–12 in solutions containing different inorganic ions, except for arborol A, which did not gel in the presence of potassium borate at concentrations around 0.1 M.

Boons and co-workers later reported the aqueous gelation of G₃-glycodendrons obtained by the parallel combination of three building blocks (monomers), which differ in the length of their alkyl chains n , as depicted in Scheme 1.³⁴ The monomers are either activated at their focal point via the deprotection of the allyl groups into phenols, or at their surface by the removal of *tert*-butyloxycarbonyl (boc) groups, followed by the reaction of the resultant amino groups with pentafluorophenyl chloroacetate. Dendrimer growth is achieved by the subsequent condensation of the chloroacetyl groups with phenol moieties to form ether linkages. Higher generation dendrimers are obtained through this repetitive two-step sequence (activation/condensation) onto which melibiose moieties are introduced to obtain water-soluble glycodendrons (Scheme 1). The G₃-glycodendrons formed thermally reversible hydrogels at concentrations as low as 0.33–1 wt %. Again, the macromonomers are dissolved in water at 80 °C, and then the solution is rapidly cooled to 4 °C. The inner and outer alkyl chain lengths n_1 and n_3 of these dendrons strongly influenced the thermal stability of the resultant hydrogels. Increasing n_1 from 3 to 5 resulted in a decrease of the gel transition temperature (T_{gel}) from 34–37 to 15–19 °C, whereas T_{gel}

Scheme 1. Synthesis of G₃-Glycodendrons³⁴

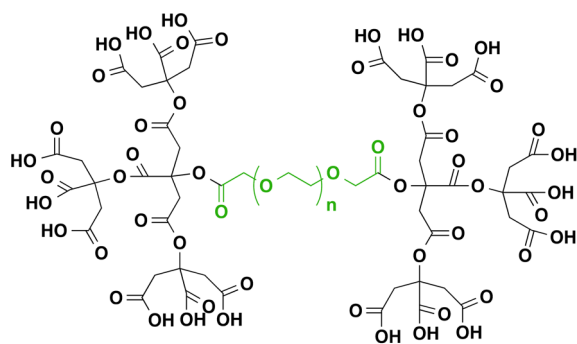
slightly rose when increasing n_3 . The inner alkyl chain length n_1 also influenced the water solubility of the hydrogelators. For example, when heated solutions of G₃-glycodendrons (80 °C) were allowed to cool to room temperature, solutions of glycodendrons with alkyl chain length $n_1 = 5$ formed precipitates, whereas those of lower alkyl chain lengths ($n_1 =$

3 and 4) formed hydrogels. Furthermore, when peripheral melibiose units were replaced with galactose groups, water-insoluble glycodendrons were obtained, demonstrating that subtle changes in the glycodendritic structures significantly impact the thermal and solution properties of the hydrogels.

Majoral and co-workers reported the physical gelation of organophosphorous dendrimers.³⁵ Polycationic G_n -dendrimers ($n = 0-4$) functionalized at their periphery with either pyridinium or ammonium chlorides formed reversible hydrogels at concentrations of 1.5–1.8 wt %, when heated in water at 60–65 °C for 11 days.

Pyridinium-functionalized dendrimers gelled faster than their ammonium counterparts, regardless of the generation considered. Replacing the chloride anions by acetates in G_1 -pyridinium-derived dendrimers decreased the gelation time of the hydrogels from 20 to 4 days, due to the bridging of the acetate anions, which likely participated in the network formation. Similarly, adding 10 to 30% of buffer (tris-(hydroxymethyl)aminomethane, TRIS), metal salts (Ni, Y, Er acetates), acids (citric, ascorbic, lactic, L-tartaric), dithioerythritol (DTE), and sodium salt of ethylenediaminetetraacetate (EDTA) to the dendritic solutions accelerated the gelation time. Freeze-fracture electron microscopy revealed that before gelation, the dendrimers appear as small dots and the texture is homogeneous, whereas after gelation, a network of aggregated dendrimers is observed. The physical interactions such as hydrogen bonding between the amide groups, π - π aromatic stacking, and hydrophobic interactions give rise to the hydrogel network.

Gitsov and co-workers reported the first synthesis of water-swelling amphiphilic dendritic-linear-dendritic (DLD) copolymers composed of PEGs as the linear hydrophilic components and poly(benzyl ethers) (PBEs) as the hydrophobic dendritic blocks.³⁶ Based on this synthetic strategy, Namazi and co-workers reported the synthesis of thermoreversible physical DLD hydrogels composed of metabolically derived citric acid synthons (CA) and PEGs (Figure 3), namely, CA-PEG-CA



[G₂]-CA-PEG-CA

Figure 3. Structure of the dendritic-linear-dendritic G_2 -CA-PEG-CA hybrid, reported by Namazi and co-workers.³⁷

hydrogels.³⁷ The G_n -CA-PEG-CA macromonomers are prepared by reacting acylated PEG chains with anhydrous CAs, followed by their subsequent reaction with activated CAs to obtain higher generations. These hybrids are not soluble in water at room temperature due to their aggregation and interaction with each other, but upon their dissolution in hot ethanol/water or dimethylformamide (DMF)/water (1:4, v/v) solutions, and upon cooling, they formed hydrogels. The $T_{\text{sol-gel}}$ of 5 wt % of CA-PEG-CA, as measured by viscometry, ranged between 40–45 and 50–55 °C for G_1 and G_2 , respectively. Moreover, the hydrogels are able to bind and solubilize small guest-molecules and are, thus, of use as potential drug delivery carriers.

In order to improve the physicochemical properties of traditional polymeric hydrogels, Zhuo and co-workers evaluated the introduction of uniform polyamidoamine (PAMAM) dendrimers to hydrogels formed with poly(vinyl alcohol) (PVA) or poly(*N*-isopropylacrylamide) (PNIPAAm).^{38,39} Upon adding a G_6 -amine terminated PAMAM dendrimer to the material and depending on the gelation process (freeze/thawing for PVA/PAMAM and at room temperature for PNIPAAm/PAMAM), an interpenetrating network (IPN) formed between the macromolecules. Infrared (IR) spectroscopy confirmed the presence of PAMAM dendrimers in the hydrogel network. The hydrogels possessed higher swelling ratios than their single component analogs, due to the increasing hydrophilicity of the PAMAM dendrimers. Moreover, PNIPAAm/PAMAM hydrogels exhibited improved temperature-responsive properties (rapid shrinking rates above the lower critical solution temperature, LCST) in contrast to traditional PNIPAAm ones, which the authors attributed to the release of water molecules from the network via the formation of water-releasing channels by PAMAM dendrimers.³⁹

An example of a strong physical dendritic hydrogel capable of self-healing when damaged is recently described by Aida.⁴⁰ The hydrogel is composed of clay nanosheets (CNSs), G_n -dendritic binders ($n = 1-3$) functionalized with guanidinium end groups, and sodium polyacrylates (ASAP; Figure 4) and is a composite

Clay nanosheets (CNS)

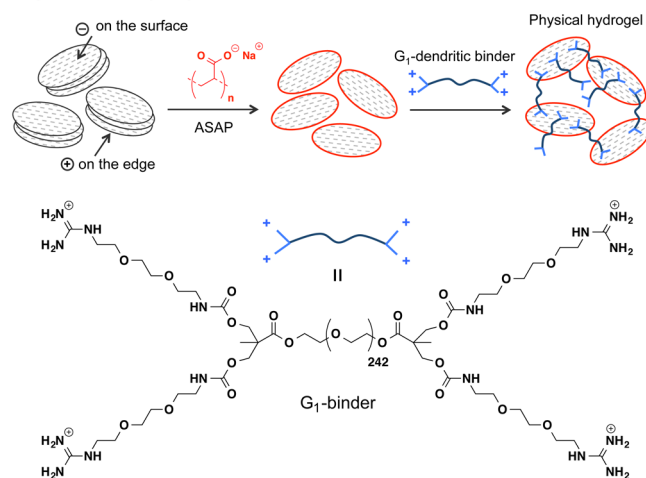


Figure 4. Schematic representation of a physical dendritic hydrogel formed by the self-assembly of CNS/ASAP/ G_1 -dendritic binder, as reported by Aida and co-workers. Adapted with permission from ref 40. Copyright 2010 Macmillan Publishers Ltd.; <http://www.nature.com/nature/index.html>.

material. Upon mixing CNSs (2%) with ASAP (0.06%) in water at room temperature, the highly entangled nanosheets are dispersed while still interacting with the anionic ASAP via their positively charged edges (Figure 4). The subsequent addition of the positively charged G_3 -dendritic binder (0.15%) to the mixture led to the formation of a cross-linked network within 3 min, due to the electrostatic interactions between the guanidinium groups of the binder and the negatively charged oxyanions present on the nanosheets surface (Figure 4). The hydrogel can also be formed without the presence of ASAP although a lower mechanical strength is obtained. When the G_n -dendritic binder is replaced by guanidinium hydrochloride,

no gelation occurred. Additionally, the telechelic structure of the dendritic binder significantly impacts the gelation process, as a monodendron version of the G_3 -binder (i.e., PEG- G_3 -dendron) did not induce the hydrogelation. The storage (G') and loss (G'') moduli are independent of the frequency at all generations ($n = 1-3$), and the resulting hydrogels exhibited an elastic response ($G' > G''$) over the entire range of frequencies. The G_3 -binder gave a hydrogel with the highest G' value among the three generations considered, due to the multivalent effect of the dendron. G' values depended on the amount of CNSs in hydrogels. For example, when increasing the amount of CNS to 5%, the highest G' value reported for supramolecular hydrogel is noted (0.5 MPa). Additionally, the hydrogels are capable of rapid self-healing when damaged and exhibit, once recovered, G' values 50 times higher than other electrolyte hydrogels with comparable recovery speed, due to the mechanical toughness of CNSs. Finally, the dendritic hydrogels are able to encapsulate and maintain the biological activity of proteins, expanding their use as carriers for biological activities. For example, the incorporation of myoglobin within the hydrogel network did not cause its denaturation after one week, and the protein maintained 70% of its activity relative to free myoglobin. This elegant strategy provides an easy and eco-friendly approach to supramolecular hydrogels with high mechanical strength and fast-recovery capability, and these materials may be of use for many biomedical applications.

Lee and co-workers developed nematic reversible hydrogels composed of penta-*p*-phenylene rods and dendritic oligoether chains (Figure 5).⁴¹ The hydrogels are able to encapsulate cells

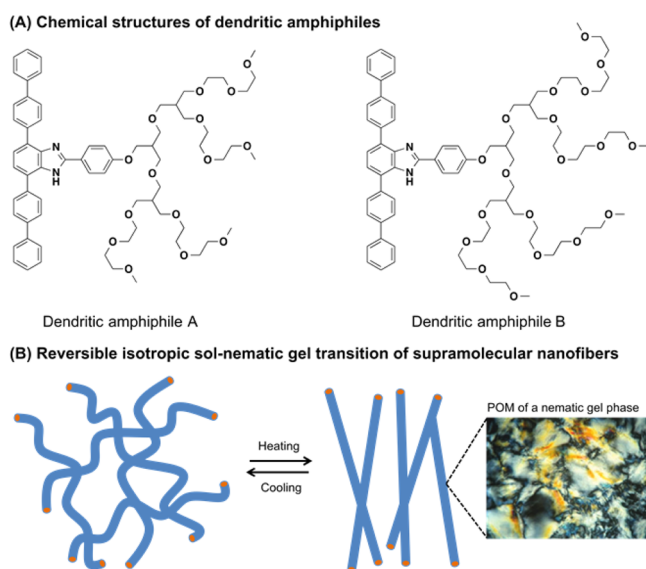


Figure 5. (A) Structures of dendritic amphiphiles developed by Lee et al., and (B) schematic representation of a reversible isotropic sol-nematic gel transition of supramolecular nanofibers. Adapted by permission from ref 41. Copyright 2011 Macmillan Publishers Ltd.; <http://www.nature.com/ncomms/index.html>; POM: Polarized Optical Micrograph.

within their matrix and enhance their proliferation without compromising cellular viability. Such materials are of interest for tissue regeneration applications. The supramolecular anisotropic 3D network is formed upon heating the dendritic structures in water to 30 °C, at concentrations greater than 0.8 wt %, causing the dehydration of the oligoether chains and the

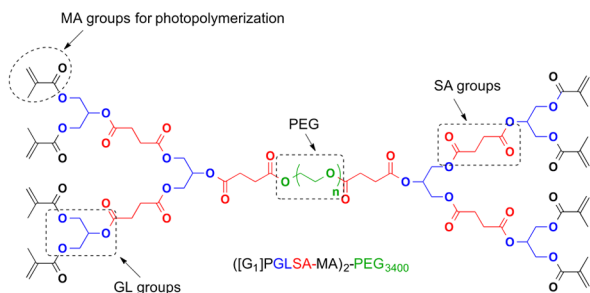
nematic alignment of the randomly oriented nanofibers via the resulting hydrophobic interactions, as observed by transmission electron microscopy (TEM). The hydrogels exhibited G' values (around 120 Pa, at 1 rad·s⁻¹) higher than G'' in the frequency range of 0.1 to 100 rad·s⁻¹. The nematic network transformed into an isotropic liquid upon cooling to 10 °C, enabling the release of encapsulated cells through a sol-gel transition.

2.2. Chemical Gelation. Covalently cross-linked dendritic hydrogels are formed when dendritic macromolecules cross-link with other similarly or complementarily multifunctional cross-linkers and form water-swellable 3D networks through the formation of covalent and nonreversible bonds (i.e., C-C, C-X, or X-X, where C is carbon and X is an oxygen, nitrogen, or sulfur; chemical gelation, Figure 1B). These bonds are obtained either by photopolymerization of dendritic macromolecules bearing photosensitive groups on their backbones with or without the presence of reactive monomers, or by condensation/addition reactions such as amidation, esterification, thioesterification, Schiff base formation, Michael addition, and other click-type reactions, between the dendritic units and other multifunctional cross-linkers, as depicted in Figure 1B. These dendritic hydrogels are usually stronger and more stable *in vivo* than their physical counterparts due to the nonreversible linkages present in their network. They are also often used for applications where extended use of the material is required before its degradation. Finally, the use of chemical gelation can afford a diverse panel of hydrogels with various physical and rheological properties through careful selection of the dendritic unit, the cross-linker type, and the cross-linking process.

An early example illustrating the gelation of dendritic macromolecules by photopolymerization is described by Grinstaff and co-workers in 2002.⁴² The hydrogel is composed of poly(glycerol-succinic acid)-poly(ethylene glycol) DLD copolymers, namely $([G_n]PGLSA-MA)_2-PEG_{3400}$, as depicted in Figure 6 (top). The hydrogel precursors contained two biodegradable dendritic units composed of glycerol (GL) and succinic acid (SA), linked by a PEG chain. These branched macromonomers are further functionalized with methacrylate (MA) end groups, which upon photopolymerization (with use of a photoinitiator and a cocatalyst) in water, cross-link and form the 3D network, in 10–30 s. The aqueous solubility of the macromonomer is imparted through the use of PEG chains, while the naturally occurring GL and SA metabolites ensured the biodegradability of the hydrogel *in vivo*.

Carbamate-linked hydrogels, composed of poly(glycerol- β -alanine)-poly(ethylene glycol) DLD copolymers, namely, $([G_n]PGLBA-MA)_2-PEG_{3400}$ (Figure 6, bottom), are also described, based on the same strategy, to ensure prolonged *in vivo* stability of the material compared to their ester-linked counterparts, described above.⁴³ For the formation of both hydrogels, buffer solutions of DLD copolymers are photo-cross-linked at concentrations of 5–20 wt % with an argon-ion laser (514 nm) in the presence of eosin-Y photoinitiator. The $([G_1]PGLSA-MA)_2-PEG$ and $([G_1]PGLBA-MA)_2-PEG$ hydrogels at 5–10 and 5–20 wt % respectively, showed minimum swelling, whereas $([G_1]PGLSA-MA)_2-PEG$ hydrogel at 20 wt % swelled the most with a weight swelling ratio percent of 12% after 30 days of incubation in phosphate buffered saline (PBS) solutions.⁴³ The rheological properties of the hydrogel scaffolds strongly depended on the macromonomer concentration with the higher concentration affording stiffer hydrogels. Specifically, the Young's modulus E and complex shear moduli G^* of the $([G_1]PGLSA-MA)_2-PEG$ hydrogels are 21 ± 2 and 1 ± 0.1 at 5

(A) Dendritic-linear-dendritic copolymer with ester linkages



(B) Dendritic-linear-dendritic copolymer with carbamate linkages

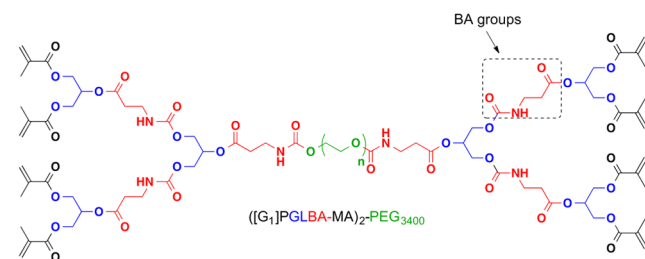


Figure 6. Structures of $((G_1)PGLSA-MA)_2-PEG_{3400}$ and $((G_1)PGLBA-MA)_2-PEG_{3400}$ dendritic-linear-dendritic copolymers, designed by Grinstaff and co-workers;^{42,43} G, generation; P, poly; GL, glycerol in blue; SA/BA, succinate (top) or β -alanate (bottom) in red; MA, methacrylate in black; PEG, poly(ethylene glycol) in green.

wt %, respectively, whereas higher values of 661 ± 13 kPa and 45 ± 3 kPa are obtained at 20 wt %, respectively. The replacement of SA with BA units in G_1 macromonomers afforded hydrogels with higher E and G^* values at both concentrations ($E = 47 \pm 1$ and 912 ± 16 kPa; $G^* = 2 \pm 0.1$ and 80 ± 2 kPa at 5 and 20 wt %, respectively).

The same group evaluated covalently cross-linked dendritic hydrogels based on thiazolidine or amide linkages formed between G_n -lysine dendrons ($n = 1-2$) bearing cysteine/amine groups on their periphery and bis-aldehyde/ N -hydroxysuccinimide ester PEG chain cross-linkers, respectively (Figure 7(1) and (2)).^{44,45} For example, upon mixing stoichiometric amounts of cysteine-terminated G_1 -dendron **A** and poly(ethylene glycol bis-propionaldehyde) (pAld-PEG-pAld (**B**); $M_w = 3.4$ kDa) at either 30 or 50 wt %, in 4-(2-hydroxyethyl)-1-piperazineethanesulfonic acid (HEPES) buffer at pH 7.4, hydrogels are formed in 3 min that exhibited viscoelastic properties (Figure 7(1)). The G^* for G_1 and G_2 -dendritic hydrogels at 30 wt % are 3.8 and 10 kPa, respectively, which is consistent with the increasing cross-linking density in higher generation (dendritic effect).⁴⁴ The G_1 -dendron **A** can also react with other types of bifunctional aldehyde-terminated PEGs such as PEG-butyr-aldehyde (bAld-PEG-bAld; **G**), and PEG-2-oxoethyl succinate (osAld-PEG-osAld; **H**), of the same molecular weight and hydrogels are formed, again, within 3 min, regardless of the polymer concentration (Figure 8).⁴⁶ Hydrogels formed between dendron **A** and PEG **B** or **G** possessed thioazolidine linkages within their networks, which are susceptible to in vivo hydrolysis. However, the reaction between cysteine residues of dendron **A** and PEG **H** generated thioazolidine linkages, which subsequently rearranged via O,N -acyl migration to form the more stable pseudoproline linkages (as depicted in Figure 8) and stable hydrogels. The authors explored these two different cross-linking chemistries in order to evaluate the effect of the

hydrogel formulation and cross-linking type on the material physical properties and degradation. The formation of thiazolidine vs pseudoproline linkages on a model substrate consisting of a cysteine methyl ester and a tetra-ethylene glycol diester-aldehyde can be followed by 1H NMR. Specifically, the appearance of the new α methylene ester proton resonance at 3.88 ppm occurred, which confirmed the thiazolidine intermediate formation. When the O,N acyl rearrangement occurred, the α methylene ester peak at 3.88 ppm disappeared and a new peak corresponding to the α methylene alcohol at 3.80 ppm appeared, confirming the presence of the pseudoproline product. Hydrogels formed between dendron **A** and PEGs **B**, **G**, and **H** degraded within 3 h, 1.5 weeks, and 6 months, respectively, confirming the higher stability of pseudoproline versus thiazolidine linkages, toward hydrolysis. Hydrogels exhibited higher swelling ratios at equilibrium with increasing wt % of polymers due to the greater amount of hydrophilic PEG chains present in the network, except for **B** PEG-hydrogels, which degraded upon swelling. Similarly, stiffer materials are obtained with increasing concentrations of polymers, with E and G^* values ranging from 20 to 1000 and 1 to 200 kPa, respectively, with initial polymer wt % of 10–50%, for all hydrogels. After swelling to equilibrium, E and G^* dropped drastically to 1–160 and 1–15 kPa, respectively, for both **G** and **H** PEG-hydrogels.

Amide-linked hydrogels prepared from linear-dendritic (LD) G_1 -lysine-PEG **C** and poly(ethylene glycol bis- N -hydroxysuccinimide ester) (NHS-PEG-NHS (**D**); $M_w = 3.4$ kDa), are formed in 1 min, and the network formation can be followed by FT-IR spectroscopy (Figure 7(2)).⁴⁵ The weight swelling ratio percent of **C/D** hydrogels at equilibrium (i.e., $(W_{eq} - W_o)/W_o \times 100$, where W_o and W_{eq} are the weights of hydrogels after cross-linking and at equilibrium, respectively) ranged from 180 to 800% and depended significantly on the macromonomer concentration and generation, with higher swelling ratios reached at lower generations and higher polymer concentrations. Moreover, **C/D** hydrogels exhibited strong elastic responses before and after swelling, for all concentrations and generations. Specifically, E and G^* increased from 40 to 300 kPa and from 4 to 25 kPa, respectively, with increasing wt % of the polymers. As expected, due to absorbed water, a decrease in the complex moduli is observed after swelling.

Recently, the on-demand dissolution of a dendritic hydrogel is described.⁴⁷ The G_1 -lysine-PEG (**E**) containing thiol end groups reacts rapidly with poly(ethylene glycol disuccinimidyl valerate) (SVA-PEG-SVA (**F**); $M_w = 3.4$ kDa) to form thioester-linked hydrogels in seconds (Figure 7(3)). The hydrogels exhibited higher G' values of 37 kPa at 30 wt % as compared to 6 kPa at 10 wt % due to the increase in polymer content and higher cross-linking density of the hydrogel. A strong elastic response ($G' > G''$, $\tan \delta < 0.1$) is observed at frequencies between 0.1 and 10 Hz. After swelling to equilibrium, G' values decreased significantly at both concentrations (0.2 and 18 kPa at 10 and 30 wt %, respectively). The on-demand dissolution feature of the dendritic hydrogel is based on the thiol-thioester exchange mechanism between the thioester linkages present in the hydrogel and an added thiolate solution. When hydrogels are exposed to various concentrations of cysteine methyl ester (0.1–0.5 M) in PBS buffer solutions at different pH (7.4 and 8.5), the dissolution time of the hydrogels decreased with increasing cysteine concentration and pH of the buffer. On the

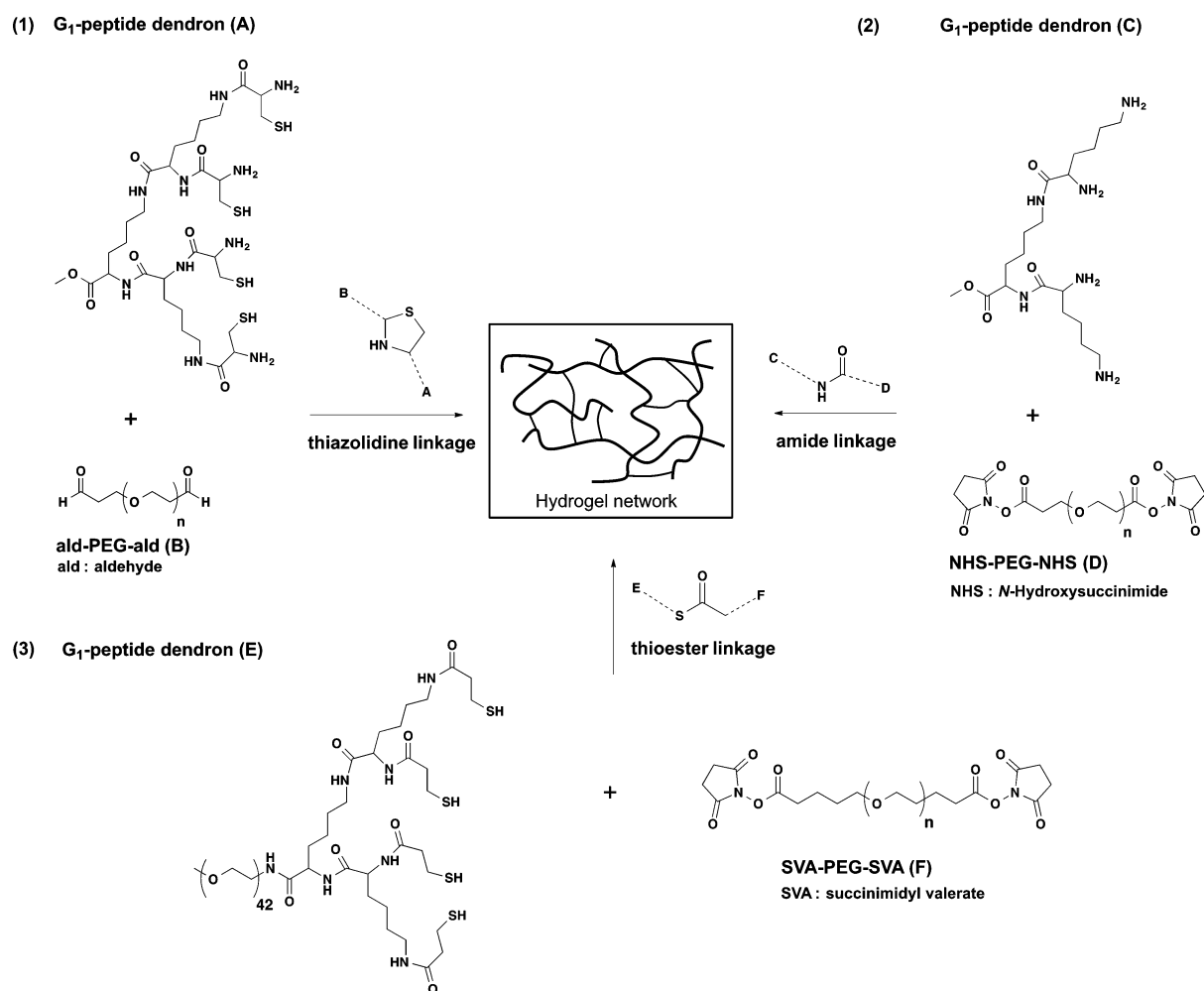


Figure 7. Examples of dendritic hydrogels based on covalent cross-linking formed via (1) thiazolidine linkage, (2) amide linkage, and (3) thioester linkage.

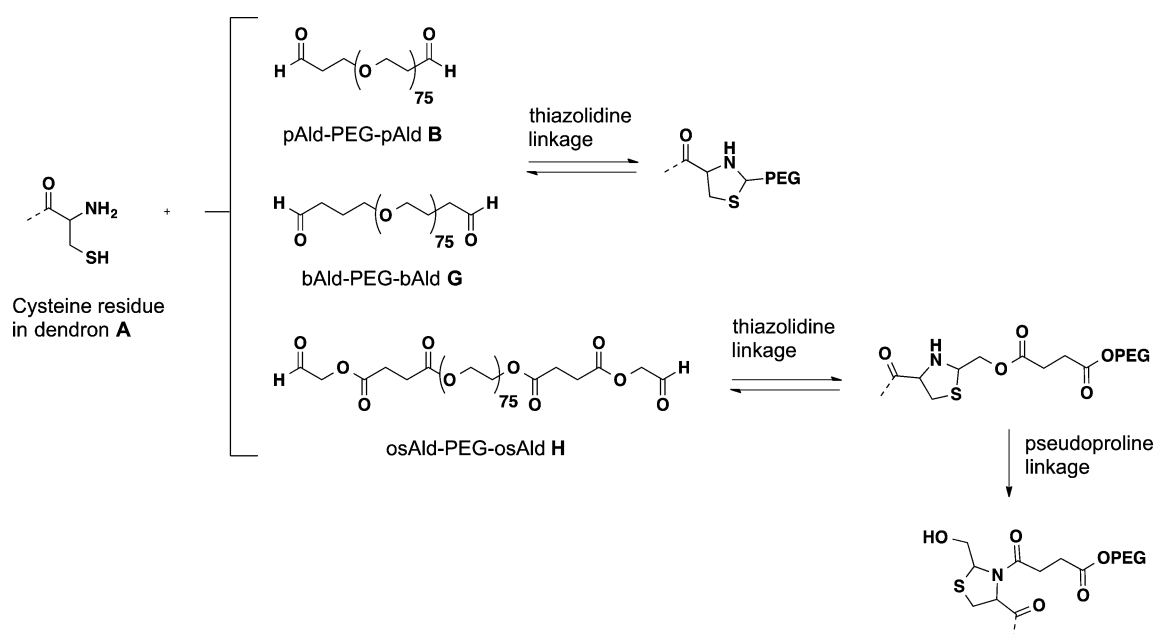


Figure 8. Reaction of cysteine residues of dendron **A** with aldehyde-derived PEGs to form either thiazolidine or pseudoproline linkages within hydrogel networks.

other hand, exposing the thioester hydrogels to a lysine buffered solution (0.3 M, pH 8.5) did not cause their dissolution, indicating that a thiol–thioester exchange reaction is responsible for the cleavage of the thioester linkages when exposed to cysteine solutions.

Gitsov and co-workers reported the synthesis of covalent amphiphilic hydrogels constructed of hydrophilic PEG chains bearing isocyanate or epoxide end groups and hydrophobic G_n -PBE dendrons ($n = 1-3$), functionalized with peripheral nucleophilic amino groups (Figure 9).^{48,49} Upon mixing the

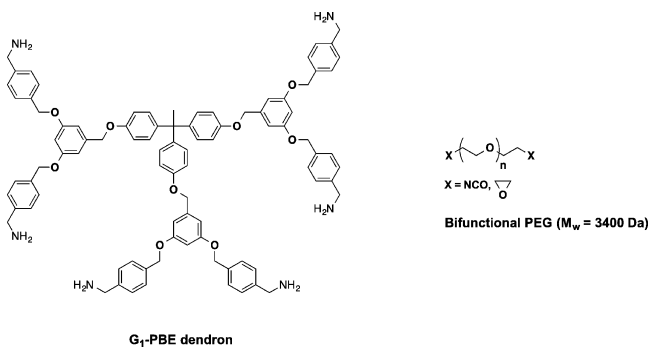


Figure 9. Chemical structures of hydrophobic (left) and hydrophilic (right) building blocks for amphiphilic hydrogel formation, as reported by Gitsov and co-workers.^{48,49}

reactive macromolecules, the hydrogels are formed by two types of chemical linkages: urea or amine, within 10 min at room temperature or 2 h at 100 °C, respectively, confirming the increasing reactivity of the isocyanate group toward primary amino functionalities in comparison to the epoxide group. The cross-linking reaction can be monitored using FT-IR microscopy where, for example, a complete disappearance of the characteristic isocyanate and primary amino groups bands at 2265 and 3370–3297 cm^{-1} , respectively, and the appearance of the urea and amide II and amide III bands, at 1700–1650, 1560, and 1240 cm^{-1} , respectively, confirmed the formation of the urea linkages within the network. Swelling measurements performed on all hydrogels showed that equilibrium swelling is reached within 10 to 30 min (swelling ratio calculated as the ratio of the weight of the swollen hydrogel to the weight of the original dry gel). Hydrogels formed between PEG-diisocyanate or PEG-bis(epoxide) and G_n -dendrons, possessed weight swelling ratios at 20 °C, in water, ranging from 4.1 to 7.8 and 2.9 to 4.1, respectively, depending on the feeding ratio and generation of dendrons. Generally, hydrogels formed with PEG-diisocyanate exhibited higher swelling ratios than those formed with PEG-bis(epoxide) due to the lower cross-linking density within their network, as the isocyanate end groups can also react with water under gel formation conditions. This example nicely highlights how the hydrogel structure, degree of cross-linking, and chemical compositions of functional groups on the dendritic surface significantly influence the physico-chemical properties of the gel. The same group also reported the synthesis of an unusual water-swellable amphiphilic pseudo-semi-interpenetrating network (pseudo-semi-IPN) for potential resin capture–release applications. The network is formed by a transesterification reaction between bifunctional PEG chains with terminal hydroxyl groups and peripheral ethyl esters of LD G_3 -PBE/PSt copolymers (PSt = poly(styrene))⁵⁰ This synthetic strategy afforded a permanent attachment of the linear polymer to the network, whereas all semi-IPNs reported

thus far potentially suffered from the extractability of their linear components, which will lead to decreased mechanical properties. The transesterification reaction was monitored by ^1H NMR, which confirmed the formation of ester linkages between the PEG and the dendritic ester. Moreover, bulk reactions afforded more densely cross-linked networks than the solution reactions between the components, and the pseudo-semi-IPNs were formed after 24 h, 3 days, and 7 days, with PEG-4K, PEG-11K, and PEG-15K, respectively. The slower gelation of higher molecular weight PEGs is likely due to the decreased mobility of longer PEG chains in bulk and the lower accessibility of the PEG–OH groups and the peripheral esters of the dendritic part for the transesterification reaction. Other characterization techniques such as DSC and SEC confirmed the formation of the interlocked semi-INP network. Finally, pyrene tags incorporated in the network demonstrated the chemical accessibility of the terminal groups in PSt linear segments for further functionalization of the material.

Another approach for the preparation of covalent dendritic hydrogels relies on the chemoselective orthogonal reaction between an alkyne and an azide (click chemistry), which occurs in high yields, in water, and at physiological conditions.⁵¹ Malkoch and co-workers successfully reported the preparation of such hydrogels starting from Trizma hydrochloride building blocks for the construction of AB_2C -type monomers (where A is a carboxylic acid, B is an alcohol, and C is an acetylene unit).⁵² The monomers are used for the growth of the multifunctional dendrimers, as depicted in Figure 10, which

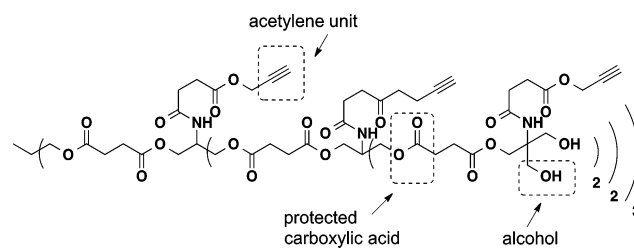


Figure 10. Structures of bifunctional dendrimers reported by Malkoch and co-workers, composed of acetylene units for click reaction and hydroxyl groups for postfunctionalization.⁵²

upon reacting with bifunctional poly(ethylene glycol bis-azides) ($\text{N}_3\text{-PEG}_{8000}\text{-N}_3$; $M_w = 8$ kDa) using a click-type procedure, formed cross-linked networks in 30 min. The G_2 -dendritic hydrogel swelled up to 96% in water, and degraded within 1 h at pH 11 and 4 days at pH 4.

The same group recently reported the preparation of other multifunctional dendritic cross-linkers.^{53,54} Similarly, the group used Trizma hydrochloride building blocks for the construction of AB_2C -type monomers where the acetylene units are replaced by either azide or alkene functionalities. The alkene groups are installed within the polymer structure to cross-link with bifunctional poly(ethylene glycol dithiols) (SH-PEG-SH) through UV initiated thiol–ene coupling (TEC) reactions, to form the dendritic hydrogels. The azide groups, on the other hand, are introduced for postfunctionalization of the cross-linkers with biological molecules through copper-catalyzed azide–alkyne cycloaddition (CuAAC) click reaction, as depicted in Figure 11. One specific example, reported by Malkoch et al., evaluated the use of two multifunctional dendrimers presenting either six azide or ene groups on the periphery, and three enes or azides on the interior of the

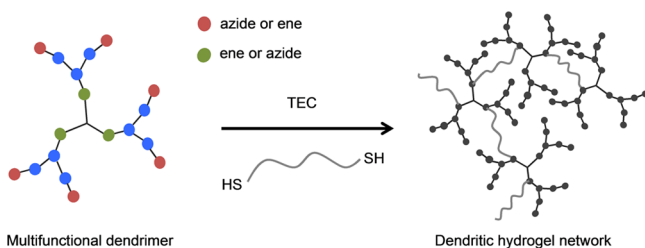


Figure 11. Schematic representation of the dendritic hydrogel formation through UV initiated TEC reaction. Adapted with permission from ref 53. Copyright 2013 Royal Society of Chemistry. For the hydrogel network: azide, on the periphery; ene, on the interior of the dendrimer backbone.

dendritic backbone, as cross-linkers for hydrogel formation.⁵³ Irradiation of the ethanol solution containing macromonomers, SH-PEG-SH ($M_w = 6$ kDa), and Irgacure 2959 photoinitiator for 10 min afforded the hydrogels. After exchanging the ethanol for water, the hydrogel containing azides on the periphery possessed a weight equilibrium swelling ratio percent of 870% and E of 21.7 ± 2.5 kPa. On the other hand, the inverted dendritic scaffold (alkenes on the periphery) exhibited an equilibrium swelling ratio percent of 780%, with higher E value of 42.8 ± 2.3 kPa.

Sanyal and co-workers reported the preparation of “clickable” hydrogels starting from G_n -DLD macromonomers, composed of two branched bis(hydroxymethyl)propionic acid (bHMPA) units functionalized with acetylene end groups, which are linked by a PEG chain (Figure 12).⁵⁵ Upon reaction of these

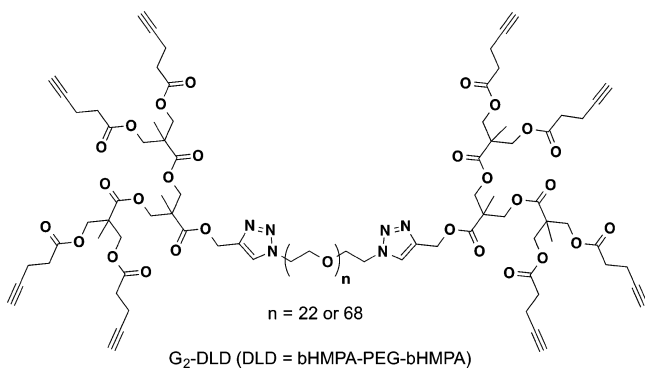


Figure 12. Chemical structure of G_2 -dendritic-linear-dendritic macromonomers functionalized with acetylene end groups, precursors of “clickable” hydrogels.⁵⁵

copolymers with bifunctional N_3 -PEG- N_3 ($M_w = 2$ and 6 kDa) via a click-type procedure, a cross-linked network is formed within 10 min, with a weight swelling ratio percent at equilibrium between 800 and 2000% (i.e., $(W_s - W_d)/W_d \times 100$, where W_d and W_s are the weights of dried and swollen hydrogels), respectively, depending on the macromonomer/cross-linker ratio and the PEG molecular weight. Through judicious choice of the equivalent ratios of the reactive groups present on the macromonomers, hydrogels can be prepared with remaining free alkyne groups for further coupling chemistry. The authors demonstrated post-hydrogel functionalization via the coupling of biotin and the subsequent immobilization of streptavidin. These results lay the foundation for hydrogels used for protein delivery or for studying the effects of specific proteins on cells that are encapsulated within

the hydrogel matrix. The same group recently reported the development of DLD hydrogels through the “metal-free” photoinitiated TEC reaction.⁵⁶ The DLD building blocks are similar to the ones previously reported by the Sanyal group (Figure 12), except that the peripheral acetylene groups are replaced with alkene units for the subsequent TEC reaction. Hydrogel precursors, dissolved in a mixture of water and ethanol, are applied between a polydimethylsiloxane (PDMS) mold and methacrylate functionalized glass surface. After exposure to UV light and removal of the PDMS mold, hydrogel patterns are formed. Residual alkene units within the network can be subsequently reacted with a BODIPY-thiol fluorescent dye after UV irradiation and photoinitiation, documenting the ability to further functionalize a hydrogel after it has been synthesized. The post-functionalization of the hydrogel depended on the DLD generation and PEG molecular weight with shorter PEG segments of the same generation exhibiting higher fluorescence intensity.

In summary, the compositional preciseness of dendrimers enables the preparation of hydrogel with specific properties as well as the development of well-defined structure–property relationships to guide further research. In addition, the high degree of functionality of the dendrimer allows the formation of hydrogel cross-links as well as the introduction of additional chemical groups for advanced functions.

3. BIOMEDICAL APPLICATIONS OF DENDRITIC HYDROGELS

The development of new dendritic macromonomer compositions along with new hydrogel cross-linking strategies is enabling the preparation of hydrogels with optimized structures and properties for their evaluation in the biomedical and bioscience fields. The following section describes selected examples of dendritic hydrogels, spanning from wound repair and tissue engineering to drug and gene delivery, where the dendritic structure plays a crucial role in optimizing the hydrogels features for the intended application.

3.1. Wound Repair. When the human body undergoes a traumatic injury requiring surgical intervention, the wound requires immediate decontamination, debridement, and effective soft tissue management to avoid infection and stimulate healing. The standard of care for simple wounds without soft tissue loss is the use of sutures to close the wound and ensure a leak-tight environment for adequate healing. Although sutures exhibit high tensile strength and a low dehiscence rate of the sutured wounds, they can cause cutaneous nerve damage resulting in scar pain, inflammatory reactions, keloidal or other abnormal scar tissue formation, and require timely removal. Early removal may facilitate wound dehiscence and promote infection, while late removal may be difficult due to skin overgrowth or induce additional trauma to the site. Moreover, suture placement is time-consuming and may require anesthesia. Therefore, biocompatible and biodegradable dendritic hydrogel adhesives may offer a useful and practical alternative to suturing in the management of wounds, because they are nontoxic, easily administered, and more importantly, the dendritic composition and structure allow the tuning and control of the hydrogel features and physicochemical properties for the application of interest.

The Grinstaff group investigated several compositions of dendritic hydrogel adhesives for the repair of corneal lacerations, which are one example of wounds caused by trauma, infection, and inflammation, and potentially resulting in



Figure 13. (Left) Photograph of a photo-cross-linked hydrogel sealant atop the letter a. (Middle) Photograph of a sealed in vivo chicken corneal laceration using a photo-cross-linked hydrogel sealant. (Right) Photograph of a repaired corneal autograft fastened with eight interrupted 10–0 nylon sutures and the pseudoproline-linked A/H hydrogel sealant.

blindness if untreated. The hydrogels are composed of photo-cross-linkable DLD macromonomers, namely $([G_n]\text{PGLSA-MA})_2\text{-PEG}_{3400}$ ($n = 0-3$), which contain natural SA and GL metabolites, and a PEG spacer, as depicted in Figure 6, top.^{42,57,58} Application of the G_n -DLD macromonomers at 20 wt % to full thickness 4.1 mm incisions in ex vivo human enucleated eyes, followed by irradiation with an argon ion laser (200 mW, 1 s pulse exposures, 50 total pulses) in the presence of a photoinitiator, afforded the formation of a transparent hydrogel adhesive on the wound site (Figure 13). Measurement of the leaking pressure (LP; i.e., maximum pressure reached before fluid leaked from the eye) for wounds closed with the hydrogel adhesives compared to a control group repaired with nylon sutures revealed the following result. Of the different generation of DLD copolymers tested ($n = 0-3$), only the $([G_1]\text{PGLSA-MA})_2\text{-PEG}_{3400}$ efficiently sealed the ocular wound and ensured a leak-tight environment, with a LP of 171 ± 44 mmHg as compared to 90 ± 18 mmHg for sutures.⁴² In vivo corneal laceration studies in a 28-day chicken eye model followed.^{57,58} Both the $([G_1]\text{PGLSA-MA})_2\text{-PEG}_{3400}$ and conventional sutures successfully sealed 4 mm full-thickness lacerations made in the eye of each animal, by postoperative day 2. However, upon histological examination of the tissues, ocular wounds treated with the dendritic adhesives presented more uniform corneal structures with less scarring than those repaired with sutures. Moreover, the adhesives exhibited no toxicity and completely disappeared by day 14, whereas sutures are present at day 28, and require subsequent removal by the physician. The $([G_1]\text{PGLSA-MA})_2\text{-PEG}_{3400}$ -based hydrogel adhesive is useful for treating other ocular wounds and, for example, successfully secured and sealed Laser-Assisted in situ Keratomileusis (LASIK) flaps, created on human eyes ex vivo.^{59,60}

The authors also assessed the efficiency of $([G_1]\text{PGLSA-MA})_2\text{-PEG}$ macromonomers with variable PEG molecular weights (M_w from 3.4 to 20 kDa) and formulations (from 10 to 40 wt %), in sealing 4 mm central corneal lacerations made on ex vivo porcine eyes. The ocular wounds were either sealed with 10, 20, and 40 wt % of $([G_1]\text{PGLSA-MA})_2\text{-PEG}_{3400}$ or 10 and 20 wt % of $([G_1]\text{PGLSA-MA})_2\text{-PEG}_{10000/20000}$ hydrogel adhesives, and the results compared to sutured treated eyes.⁶¹ The groups treated with the adhesives exhibited higher LPs than those repaired with sutures, at all formulations and concentrations. Additionally, at a constant molecular weight, greater LPs and hydrogel adhesion to the tissue are obtained at higher macromonomer concentration. Finally, increasing the PEG molecular weight from 3.4 to 10 kDa resulted in increased

LPs at the 10 and 20 wt % macromonomer concentration. Further increase of the molecular weight up to 20 kDa PEG spacer of the macromonomer resulted in a decreased LP.

Another example of surgical wounds where the use of DLD-based hydrogel adhesives is advantageous over sutures is in a corneal transplant procedure or penetrating keratoplasty (PKP). In a PKP, a full-thickness section of tissue is removed from the damaged cornea and replaced by a healthy corneal tissue from a donor, which is manually sutured to the recipient corneal rim. This procedure presents complications such as delayed visual recovery, surgically induced astigmatism, eye infection, inflammation, and tissue damage, often related to the use and removal of sutures. A sutureless corneal transplantation would be ideal to overcome the drawbacks mentioned above. Toward this goal, $([G_1]\text{PGLSA-MA})_2\text{-PEG}_{3400}$, $([G_1]\text{PGLSA-MA})_2\text{-PEG}_{10000}$, and $([G_1]\text{PGLSA-MA})_2\text{-PEG}_{20000}$ -based hydrogel adhesives are evaluated for supplementing corneal transplant procedure by reducing the number of sutures used to secure the donor corneal transplant.⁶¹ In an ex vivo porcine model, the dendritic adhesive (20 wt %) is first applied on autografts already sealed with 16 or 8 interrupted 10–0 nylon sutures, and the LPs are measured and compared to suture-treated controls. For autografts pretreated with 16 interrupted sutures, all three formulations exhibited LPs above 100 mmHg, which are higher than the control group of suturing alone (50 mmHg). For autografts pretreated with eight interrupted sutures, on the other hand, the adhesive possessing the lower molecular weight PEG exhibited the lowest LP among the three formulations tested (40 mmHg as compared to 80 mmHg for the other two); however, all formulations performed better than the control group (5 mmHg). The $([G_1]\text{PGLSA-MA})_2\text{-PEG}_{10000}$ and $([G_1]\text{PGLSA-MA})_2\text{-PEG}_{20000}$ -based hydrogel sealants are more efficient in securing corneal transplants with minimum sutures than $([G_1]\text{PGLSA-MA})_2\text{-PEG}_{3400}$ alone, and successfully prevented the eye from leaking at high pressures. Moreover, these hydrogels acted as a barrier for postoperative microbial infections since they tightly close the wound once they adhered on the tissue.

Hydrogel adhesives formed directly on the wound site through photopolymerization of dendritic macromonomers are convenient and yield efficient adhesives or sealants for the repair of ophthalmic wounds. However, alternative cross-linking strategies that do not require the use of light or additives for network formation are also of interest, if they could be formed chemoselectively and under physiological conditions. The Grinstaff group identified several cross-linking strategies to give linkages, such as thioesters, amides, and

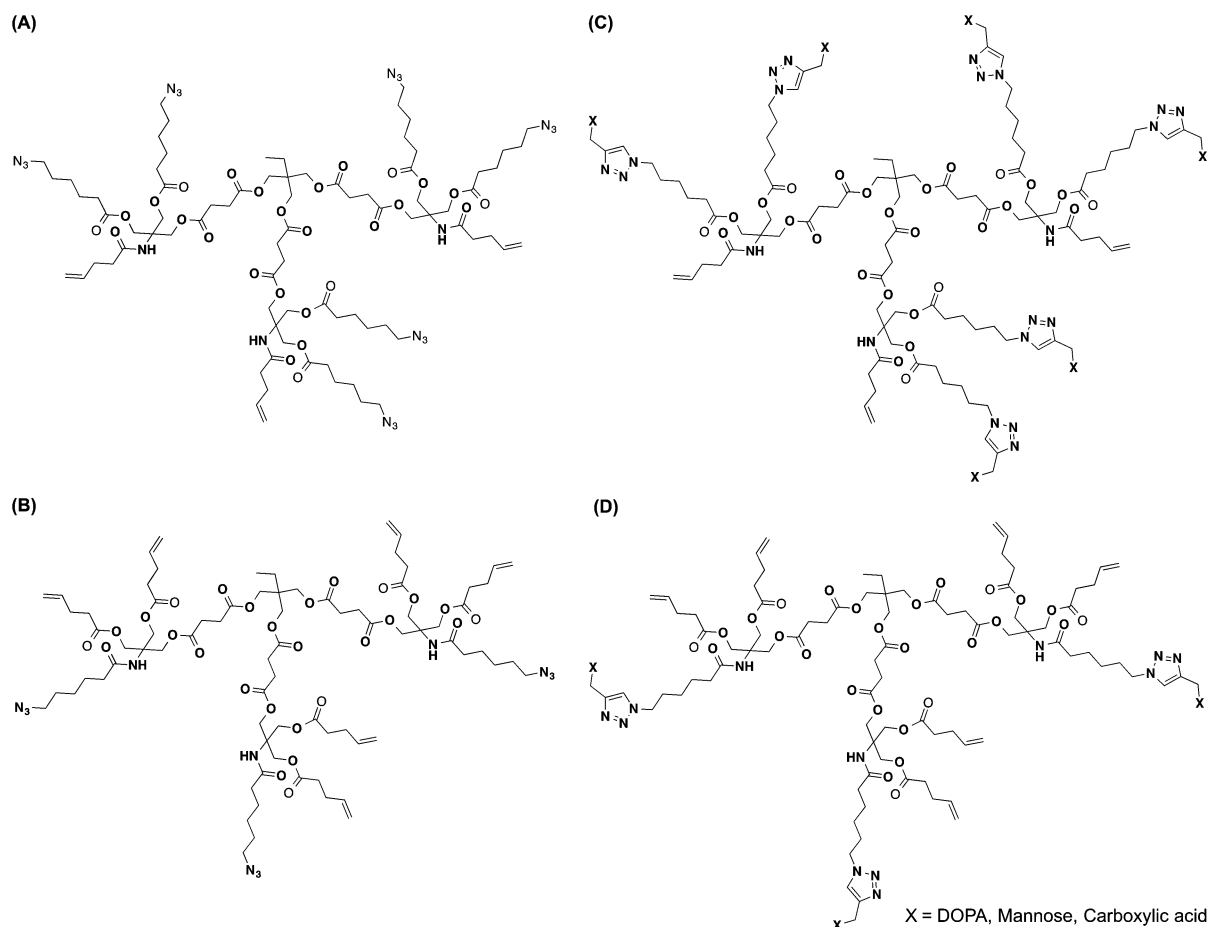


Figure 14. G_1 -trizma-based dendritic cross-linkers evaluated as adhesive primers in FRAPs for the fixation of fractured bones. Adapted with permission from ref 53. Copyright 2013 Royal Society of Chemistry.

thiazolidines, which can be formed between biocompatible peptide dendrons and bifunctional PEG chains, in water, at room temperature and physiological pH, without the generation of toxic byproducts, as depicted in Figure 7.

For example, a two-component A/B hydrogel adhesive formed from the cross-linking of cysteine-terminated peptide G_1 -dendron **A** and pAld-PEG-pAld **B** (Figure 7(1)) is described for securing 3 mm clear corneal incisions made on ex vivo enucleated eyes.⁴⁴ The precursor macromonomers are mixed together at room temperature and quickly applied on the incision, and the LP is measured and compared to those obtained with self-healed and suture-repaired incisions. The hydrogel sealant completely adhered to the wound site and successfully closed corneal incisions with higher LPs of 184 ± 79 mmHg than self-healed and suture-repaired eyes (24 ± 8 and 54 ± 16 mmHg, respectively). The adhesive is easily prepared and can be applied on the wound site, does not inflict additional tissue trauma nor requires the use of additives or light sources to form the cross-linking network in situ.

Another ex vivo wound model investigated with the A/B hydrogel adhesive was an 8.5 mm LASIK flap with a 180 mm depth plate.⁶⁰ Specifically, the hydrogel precursors at 55 wt % are mixed and applied around the wound edges. Gelation occurred within 30 s to give a closed wound. Similar to the photopolymerized G_1 -DLD-based hydrogels discussed above, the thiazolidine-linked hydrogels adequately adhered to the tissue and efficiently secured LASIK flaps. Moreover, the hydrogel provided a tight seal at the tissue interface, confirmed

by injecting fluorescein dye under the flap, ensuring that no leakage occurred around the flap edge. These wounds like the above corneal lacerations heal rapidly within 2–5 days, and thus, long-term hydrogel stability is not required.

The authors evaluated the more stable pseudoproline-linked A/H hydrogel adhesives (Figure 8) in securing large corneal wounds such as corneal transplants where extended time performance of the sealant is required for adequate healing.⁶² After transplanting new corneal tissue from an organ donor into the damaged original cornea, the host–graft tissue interface is either secured with 16- or 8-interrupted 10–0 nylon sutures, sutures and hydrogel sealant, or hydrogel sealant alone. The study also evaluated whether the pseudoproline-linked hydrogel sealant could efficiently aid sutures in securing the transplanted tissue until the wound was healed, thus minimizing the number of sutures or if it could seal and secure a PKP on its own. The LPs for the autografted eyes are measured following the same experimental protocol reported for corneal lacerations. The autografted eyes treated with 16-interrupted 10–0 nylon sutures exhibited LPs of 13 ± 5 mmHg, whereas higher LPs of 63 ± 7 mmHg are reached with the ones treated with 16-interrupted sutures and the hydrogel sealant (33 wt %). Higher LPs of 101 ± 5 mmHg are obtained when the hydrogel sealant concentration is increased to 50 wt %. On the other hand, autografted eyes treated with 8-interrupted 10–0 nylon sutures exhibited LPs of 5 mmHg or less, whereas when treated with sutures and the hydrogel sealant (33 wt %), it only reached 45 ± 6 mmHg. In order to strengthen the seal on the wound, a

higher concentration of the sealant (50 wt %) is necessary to increase the LP to 77 ± 5 mmHg (Figure 13). However, at any concentration, the pseudoproline-linked hydrogel did not adhere strongly enough to the tissue in order to efficiently secure and seal the wound by itself, although it can act as a physical barrier when applied on the wound interface to prevent it from postoperative infections.

The same group also evaluated the use of C/D hydrogel sealants formed via the cross-linking of amine terminated- G_1 -lysine dendrons C and NHS-PEG-NHS D for repairing scleral incisions used in pars plana vitrectomy procedures (Figure 7(2)). Vitrectomy is a surgical procedure to remove the vitreous humor in the eye in order to address vision problems caused by retinal detachment, macular holes, or vitreous hemorrhage. After making tiny incisions in the pars plana of the eye to conduct the vitrectomy, the surgeon withdraws the vitreous gel and repairs the retina, then refills the eye with a saline solution to restore and maintain the normal IOP and closes the incisions with sutures until the wound is healed. To determine whether the dendritic hydrogels offer advantages over sutures in a vitrectomy procedure, 1.4 mm scleral wounds, made in ex vivo enucleated pig eyes, are either treated with the C/D hydrogel or suture. The hydrogel precursors, mixed at 18 wt %, are quickly applied to the wounds, and the LPs are measured after gelation and compared to 7–0 Vicryl suture-treated eyes. The hydrogel adhesive adhered strongly to the host tissue via the formation of an interpenetrating network between the polymers and the tissue. The wounds treated with the hydrogel adhesives secured the incisions without any leakage at pressures as high as 250 mmHg, whereas the ones treated with sutures had lower LP values of 140 ± 68 mmHg.

Recently, the first example of a dissolvable hydrogel-based wound sealant for trauma care was reported.⁴⁷ The hydrogel contained thioester linkages (Figure 7(3)), which can be cleaved upon exposure to a thiolate solution via a thioester-thiol exchange mechanism, causing the dissolution of the hydrogel. This interesting feature is useful for the development of hemostatic adhesives, where the material is first applied on a bleeding wound in an emergency setting to secure it and limit hemorrhage and dissolved at a later time to re-expose the wound for definitive surgical care. Specifically, thiol-terminated peptide dendrons (E) and NHS-PEG-NHS (F) are quickly mixed at 30 wt % and applied on 2.5 mm incisions made on ex vivo bovine jugular veins. The thioester hydrogel formed in seconds and completely secured the punctures at pressures higher than 250 mmHg. Subsequent application of a cysteine methyl ester solution resulted in the dissolution of the hydrogel and wound leakage.

Clickable dendritic cross-linkers functionalized with azide/triazine and alkene groups are recently reported as adhesive primers for the stabilization and repair of fractured bones (Figure 14).⁵³ The dendritic primers are incorporated in composite materials (a fiber reinforced adhesive patch (FRAP)), composed of thiol-ene based matrices for further cross-linking with the adhesive primers, and E-glass fiber layers for reinforcement of the materials adhesive strength (Figure 15). The FRAP is applied on the outside of the fractured bone site to avoid its interference with the natural healing process and increase its adhesion to the bone surface area.

The dendritic structures consisted of G_1 -trizma-based macromonomers, further functionalized with adhesive peripheral units such as DOPA and carboxylic acids (CO_2H) to increase their binding to wet bones and alkene groups for cross-

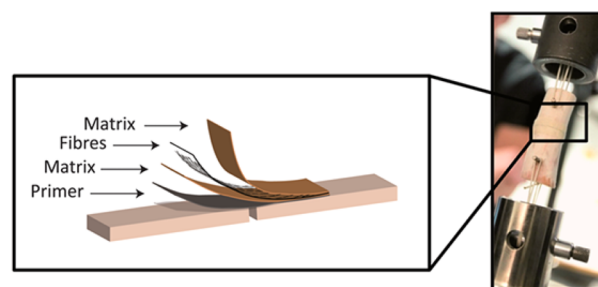


Figure 15. Representation of the FRAP on bone. Reproduced with permission from ref 53. Copyright 2013 Royal Society of Chemistry. Part of the figure adapted with permission from ref 77. Copyright 2010 American Chemical Society.

linking with the matrices upon UV activation via a TEC reaction. These primers are evaluated in FRAPs for the fixation of bones and their shear strengths are compared to FRAPs without any primer. Specifically, the free-primer FRAP exhibited a lower shear strength than all dendritic-based ones. Surprisingly, FRAPs containing dendrimer C with six DOPA and CO_2H units on the surface exhibited the lowest shear strengths of 0.6 and 0.8 MPa, respectively, of all tested dendrimers (Figure 14), whereas dendritic primers D with lesser DOPA and CO_2H adhesive groups on the surface resulted in higher shear strengths of 3.2 and 1.8 MPa, respectively. However, none of these polar triazine functional primers possessed an adhering strength equivalent to the commercial wound sealant Histoacryl (3.8 MPa). Finally, switching the triazine units in dendritic primers to azides resulted in FRAPs with higher shear strengths of 3.0 (primer B, Figure 14) and 4.2 MPa (primer A, Figure 14), attributed to the rearrangement of azides into imines and nitrogen upon irradiation and their subsequent reaction with each other to generate higher molecular weight primers capable of efficiently binding to wet bone surfaces. Furthermore, imines can hydrolyze to aldehydes in the presence of water, or form hydrates, and/or acetals, which can react with amino groups of proteins present in extracellular matrices (ECMs) and reinforce the binding strengths of FRAPs on wet bones. Neither the FRAP nor the trizma-based dendrimers exhibited toxicity to MG63 osteoblast cells, and these composite materials based on dendritic cross-linkers constitute an exciting and promising strategy for bone fixation applications.

3.2. Tissue Engineering. Hydrogels are also evaluated as scaffolds for tissue engineering because they mimic some of the aspects of the natural tissue extracellular matrix, are produced under physiological conditions, and can be easily administered to the desired site. Consequently, these materials have found their application as scaffolds for cell encapsulation and proliferation while stimulating the growth of the desired tissue, space filling agents, and vectors for bioactive molecule delivery. Natural or synthetic linear polymers are commonly used to form these hydrogels, and depending on their nature and cross-linking type, they impact the physical (i.e., gel formation and its mechanical and degradation features), the mass transport (i.e., transport of gases, nutrients, proteins, cells, and waste products within the hydrogel and from the hydrogel to the surrounding media), and the biological (i.e., absence of toxicity and immune responses, cell adhesion) properties of the hydrogel.⁶³ Recently, dendritic cross-linked hydrogels have been investigated for tissue engineering applications. These macromonomers are uniform and possess defined and controlled sizes, viscosities,

and number of multivalent cross-linking units within their structures, which allow the development of hydrogels with reproducible and adequate properties for specific applications, as highlighted in [Wound Repair](#).

The Grinstaff group evaluated the GL and SA-based dendritic photo-cross-linkable macromonomers for cartilage repair.⁶⁴ Specifically, $([G_1]PGLSA-MA)_2-PEG_{3400}$ DLD copolymers afforded highly cross-linked hydrogels with low swelling ratios due to the dendritic structure, which favored their use in confined areas such as cartilage without causing any tissue damage. Moreover, the hydrogels are able to encapsulate chondrocytes without any signs of dedifferentiation or morphological deformation and support their proliferation, as well as the production of cartilaginous protein-rich ECM in vitro. Lower concentrations (7.5 wt %) of hydrogels afforded better ECM synthesis and faster degradation of the material (5–6 weeks) than the ones with higher concentrations (15 wt %), where longer absorption time (12 weeks) resulted in a delay in cell proliferation and matrix formation.

Subsequently, the same group reported the development of similar photo-cross-linkable $([G_1]PGLBA-MA)_2-PEG_{3400}$ macromonomers ([Figure 6](#), bottom), where SA units were replaced by BAs in order to generate carbamate-linked hydrogels upon photopolymerization.⁴³ These hydrogels showed greater stability toward hydrolysis, as well as higher E and G^* values than their ester-linked counterparts, at macromonomer concentration between 10 and 20 wt %. Additionally, the hydrogels did not show any significant swelling in the concentration range of 5–20 wt %, which is ideal for their use as scaffolds for the repair of defects in in vivo confined areas such as bone and cartilage sites. Therefore, full-thickness osteochondral defects were made in medial femoral condyles of white rabbits and subsequently filled with 10 wt % of the carbamate macromonomer and quickly photopolymerized in situ to obtain the hydrogel. The defect is efficiently filled and remained intact during the entire course of the pilot study (6 months). Histological examinations of the knees after animal sacrifice showed that even without the use of implanted cells, the scaffold promoted the production of collagen II and glycosaminoglycans (GAGs) in the defects, whereas the untreated defects showed collagen I and minimal GAG production. These examples demonstrated once more the capability of dendritic structures in controlling and optimizing the hydrogels properties, where a facile tailoring of the dendrimer concentration, structure, and generation provided scaffolds with specific physicochemical, mechanical, and degradation properties for tissue engineering.

Jia and co-workers reported the preparation of a photo-cross-linkable dendritic hydrogel as a mimic of ECM, composed of two components: a linear copolymer of poly(lactic acid)-*b*-poly(ethylene glycol)-*b*-poly(lactic acid) with acrylate end-groups (PLA-PEG-PLA), and a G_4 -PAMAM dendrimer containing peripheral PEGs with terminal arginine-glycine-(aspartic acid)-(D-tyrosine)-cysteine (RGDyC) and acryloyl groups ([Figure 16](#)).⁶⁵ The introduction of PAMAM dendrimers to the linear copolymers afforded hydrogels with higher mechanical properties and degradation times and lower swelling ratios, when compared to nondendritic PLA-PEG-PLA hydrogels, due to the multivalent cross-linking units of the dendrimer. Scaffolds with low swelling ratios are useful in confined areas of the body as highly swollen materials can cause nerve damage and tissue compression and detach from the wound site. Finally, the peripheral bioactive RGDyC end

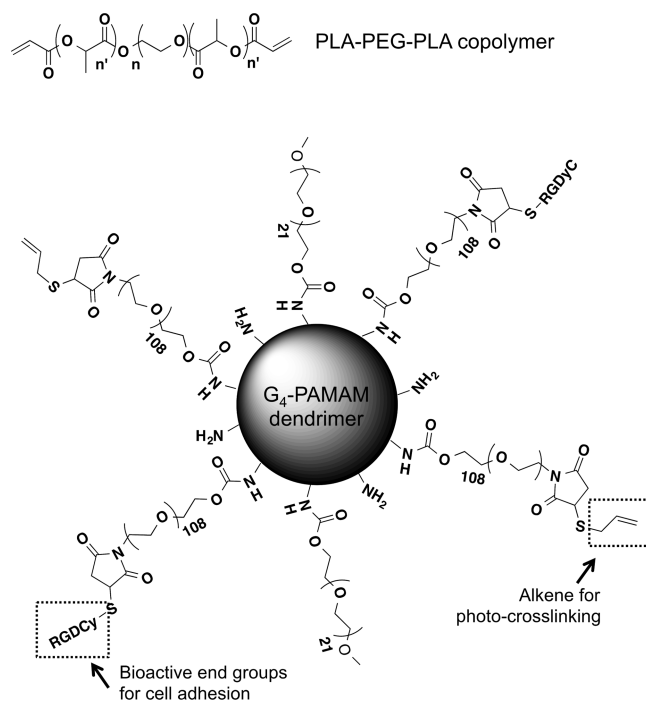


Figure 16. Precursors of the photo-cross-linkable dendritic hydrogel for tissue engineering.⁶⁵

groups increased mouse bone marrow mesenchymal stem cell (mMSC) adhesion and proliferation within the hydrogel network, and the dendritic hydrogel did not show any cytotoxic effect in vitro. As the RGDyC can trigger the activation of $\alpha_5\beta_1$ integrin receptor in mMSCs promoting osteogenic differentiation, this strategy can be used for bone tissue regeneration. Therefore, the expression of osteogenic markers such as alkaline phosphatase (ALP), osterix (OSX), parathyroid hormone 1 receptor (PTH1R), and osteocalcin (OC) was evaluated in dendritic hydrogels with and without RGDyC, using real-time polymerase chain reaction (PCR). As expected, an enhanced expression of these markers by encapsulated mMSCs is detected in hydrogels containing bioactive units. These results support the use of dendritic hydrogel scaffolds for tissue engineering, as the dendritic macromonomers ensured higher stiffness of the material and extended degradation time, and allowed the introduction of multivalent bioactive units essential for cell adhesion, proliferation, and differentiation.

Physically cross-linked dendritic hydrogels are also described for tissue regeneration applications.⁴¹ The hydrogels are composed of self-assembled dendritic nanofibers with nematic liquid crystal phases, as previously described in [Section 2.1](#) ([Figure 5](#)), and investigated as artificial mimics of natural ECMs. As a first step toward this goal, C2C12 (myoblast, mouse muscle adherent cells) cells are encapsulated in the dendritic hydrogel and the cells remained viable for at least 5 days. Moreover, the cells proliferated in colonies within the cross-linked network as opposed to monolayers as seen in tissue-culture plastics (2D), demonstrating their ability to grow in a 3D environment. Finally, due to the reversible nature of the hydrogel, the cells can be completely released from the hydrogel upon cooling, demonstrating the potential use of these scaffolds in tissue engineering applications.

3.3. Drug Delivery. Dendritic hydrogels are also investigated for drug delivery applications, due to their biocompatibility and biodegradability as well as the presence

of dendritic macromonomers, which provide high loading and solubility of the drugs within their structures and ensure their sustained release at the desired tissue site.

Kanan and co-workers recently reported the in situ development of injectable and biodegradable dendritic hydrogels formed by the cross-linking of thiopyridyl functionalized PAMAM dendrimer $[(\text{NH}_2)_{49}\text{-G}_4\text{-(NH-PDP)}_{15}]$ with 8-arm thiol terminated PEG ($M_w = 20$ kDa) for sustained intravaginal delivery of amoxicillin to treat ascending genital infections during pregnancy.⁶⁶ The 3D network formed within 10–30 s via the formation of disulfide bridges between the dendrimer and the multifunctional PEG (Figure 17). To avoid protein

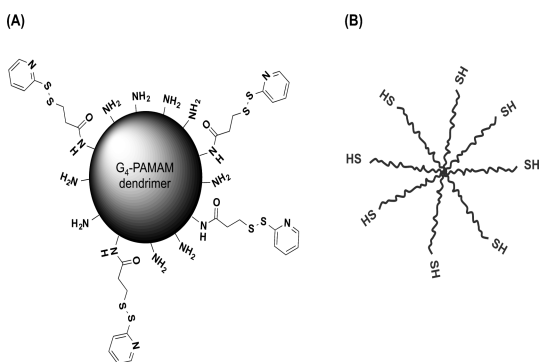


Figure 17. Pictorial representations of (A) G_4 -PAMAM dendrimer functionalized with thiopyridyl groups and (B) 8-arm PEG-SH.⁶⁶

adsorption to the hydrogel surface, PEG is introduced as one of the multifunctional macromonomers. Amine-terminated PAMAM dendrimers, on the other hand, are known to exhibit antibacterial properties against *E. coli*, *P. aeruginosa*, and *S. aureus* by disrupting the bacterial cell membrane causing cell lysis. Thus, they hypothesized that a PEGylated PAMAM hydrogel encapsulating an antibiotic (amoxicillin) would reduce the in vivo cytotoxicity of the material while maintaining the dual antibacterial activity, resulting from the in vivo sustained release of the drug as well as the released PAMAM dendrimer from the degrading hydrogel. Amoxicillin release is formulation dependent and in the three hydrogel formulations (3, 6, and 10 wt %) evaluated, a slower drug release is observed at high macromonomer concentration due to the higher cross-linking density of the hydrogel (i.e., 50% of drug amount released at 260 h for 10 wt % hydrogel as compared to 60 and 70% for 6 and 3 wt % hydrogels, respectively). Based on these in vitro results, the 10 wt % hydrogels were used in an in vivo pregnant guinea pig model. Glycerin, polyvinylpyrrolidone (PVP), and PEG₆₀₀ additives are added to the precursors solutions prior to hydrogel formation to avoid dehydration and brittleness of the material as well as to increase its mucoadhesion properties in vivo. Hydrogels injected into the cervicovaginal region are retained in this region for the whole course of the study (72 h). They slowly degraded in vaginal fluid at pH 4, with no penetration of the hydrogel or released dendrimer into the fetus membrane, which supported the use of such hydrogels for the local treatment of genital infections in pregnant women without adverse effects to the fetus. Importantly, the hydrogels are well tolerated by the animals with no change of vaginal pH, and no signs of edema or irritation observed in vaginal tissues.

Yang and co-workers described the use of G_3 -PAMAM dendrons and acrylated PEGs for the formation of photo-cross-linked hydrogels for ocular drug delivery (Figure 18).⁶⁷ Again,

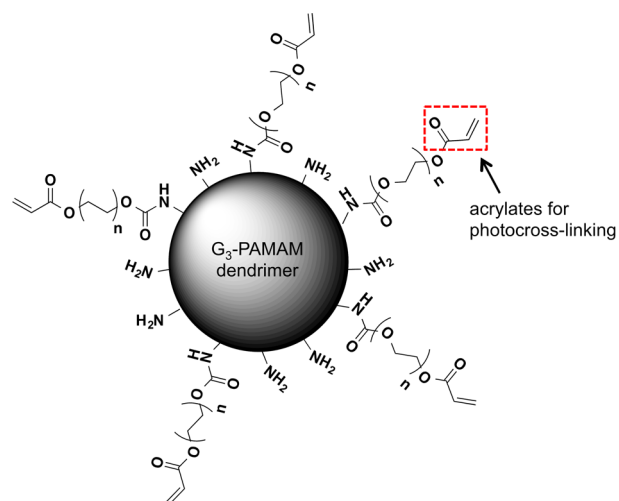


Figure 18. Pictorial representation of a photo-cross-linkable PAMAM-PEG dendrimer.⁶⁷

PEG is introduced into the formulation to increase the cytocompatibility of the material as well as its hydrophilicity, in order to accommodate the hydrophilic timolol maleate drug within the network. The amine-terminated PAMAM dendrimer is used to encapsulate the hydrophobic brimonidine drug within its hydrophobic interior structure and thus increase its solubility and loading in the hydrogel, as well as for its bioadhesive properties (interaction with negatively charged corneal surfaces). Both drugs are commonly used in eye drop formulations for the treatment of glaucoma, a condition that can cause optic nerve damage, associated with an IOP increase, and lead to blindness.

PAMAM/PEG (PP) hydrogels (8.1 wt %) are formed upon photopolymerization of acrylate groups on the periphery of the PEG chains, and the remaining positive charges of the PAMAM dendrimer interacted with the negatively charged mucin particles, as shown by zeta potential measurements, suggesting a possible increase of the material's adhesion to corneal surfaces. In vitro cytotoxic assays showed that hydrogels are not cytotoxic to human corneal epithelial cells (HCET). As expected, the encapsulation of the hydrophobic brimonidine drug within the dendritic scaffold increased significantly its solubility from 392 $\mu\text{g}/\text{mL}$ in PBS to 696 $\mu\text{g}/\text{mL}$ in hydrogels, demonstrating the advantage of dendrimer formulations in enhancing drugs loading. Furthermore, both hydrophilic and hydrophobic antiglaucoma drugs exhibited in vitro sustained releases from the hydrogels (56 and 72 h for timolol maleate and bimonidine, respectively) as compared to drugs in eye drop formulations (90 min for both drugs) due to the encapsulation of the molecules in the PEG network and dendritic core, which, if applied in vivo, would provide longer drug bioavailability and duration of activity. Similarly, drugs released from the hydrogel scaffolds exhibited higher cellular uptake by HCET cells and enhanced transcorneal transport in ex vivo bovine eyes than the eye drop solution formulations. In particular, higher levels of timolol maleate released from the gel are observed in bovine corneal epithelium, stroma, and endothelium, as compared to brimonidine and eye drop solution formulations, where no significant difference is observed after 1 h of application on the corneal surface.

The same group reported shortly afterward an advanced version of the dendritic hydrogel, composed of G_3 -PAMAM

dendrimer/poly(lactic-co-glycolic acid) (PLGA) nanoparticles and acrylate PEGs, which improved the drug delivery by extending the drug release rate on the corneal site, thus reducing frequent dosing.⁶⁸ Biodegradable PLGA nanoparticles (PLGA-NPs) are included in the scaffold as primary carriers for drug loading, whereas the dendritic hydrogel allowed the dispersion of the loaded nanoparticles within the network, as depicted in Figure 19. Unlike the previously reported dendritic

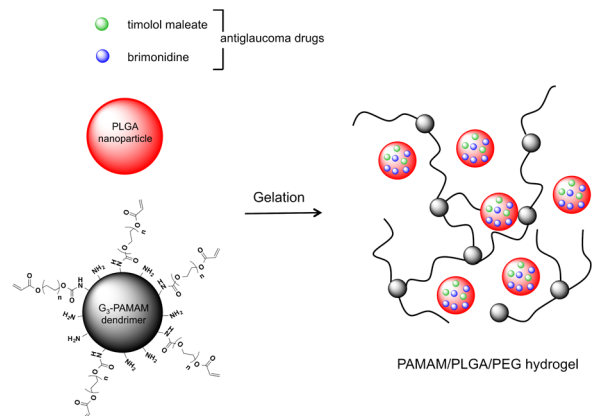


Figure 19. Composition of PAMAM/PLGA/PEG hydrogel encapsulating antiglaucoma drugs, as described by Kompella et al. Adapted with permission from ref 68. Copyright 2012 American Chemical Society.

scaffold (PP hydrogel), which is applied as a solidified hydrogel network on cornea, this composition is partially cross-linked to afford viscous solutions for use in eye drop formulations. The use of PAMAM/PLGA/PEG (PPP) hydrogels reduced significantly the IOP during 4 days in an in vivo eye rabbit model, after a single eye drop application on the cornea, whereas PP hydrogels and PLGA-NPs maintained this reduction for only 48 h, and the brimonidine/timolol maleate saline formulation for 6 h. Furthermore, both antiglaucoma drugs released from PPP hydrogels demonstrated an enhanced absorption in aqueous humor and cornea, and timolol maleate in conjunctiva, in comparison to PP hydrogels.

PLGA-NPs released from PPP hydrogels exhibited higher uptake in epithelial cells than PLGA-NPs in saline solution (e.g., 26.1% increase after 1 h incubation). The in vitro release of both drugs is extended in PPP hydrogels and PLGA-NPs as compared to the drug release from PP hydrogels and saline solutions (100% of drug released in 90 min, 48–72 h, 28 days, and 35 days for saline solutions, PP hydrogels, PLGA-NPs, and PPP hydrogels, respectively), which matched with the extended drug efficacy in vivo. Additionally, as observed by fluorescence, PPP hydrogels exhibited higher residence time on the surface of rabbit eyes as compared to saline solutions, due to the mucoadhesive properties of PAMAM dendrimers. Finally, as demonstrated by in vitro cytotoxicity assays and histological examinations of ocular tissues after sacrifice, none of the formulations are toxic to cells, or induced inflammation and discomfort, or showed any signs of morphological changes in cornea or conjunctiva.

3.4. Gene Delivery. Therapeutic genetic materials (e.g., plasmid DNA (pDNA), and siRNA) are usually delivered to the desired site of action (diseased sites or specific cell populations) within a delivery system, which protects the genetic material from fast degradation and in vivo elimination,

as well as ensures an efficient and targeted sustained gene delivery. These delivery systems are commonly composed of synthetic cationic lipids, linear polymers, or dendrimers, which bind with anionic nucleic acids (NA) via electrostatic interactions and form lipoplex, polyplex, dendriplex, or nanoparticles (NPs), respectively.^{69,70} However, despite the advantages of using such systems over administering NAs directly, low specific cell targeting of the charged particles, along with low gene transfection efficiency, represent some of the key limitations of these gene delivery vectors when utilized in vivo. There are some recent successes in using cationic lipids, identified from large screening exercises.^{71–73} While dendrimers such as PAMAMs and polypropyleneimines (PPIs) are widely explored for gene delivery, even though their application was mainly focused on their use for local or ex vivo administration,⁷⁴ few examples of dendritic hydrogels as gene delivery systems are reported in the literature, and they are primarily based on the formation/introduction of dendriplexes within the hydrogel network for sustained gene delivery.

Specifically, Zhang and co-workers recently reported the use of PEG-G₃-PAMAM dendrons (Figure 20) for the condensa-

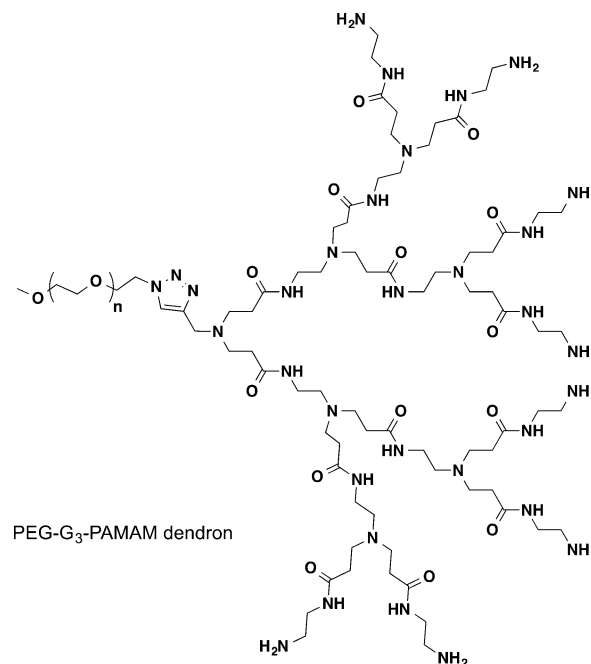


Figure 20. Chemical structure of PEG-G₃-PAMAM dendron used for the complexation of pDNA.

tion of pDNA into NPs. These NPs were further encapsulated in the hydrogel network formed via the physical cross-linking of α -cyclodextrins (α -CDs) with the PEG segments of the LD hybrid and the subsequent formation of the inclusion complexes.⁷⁵ The in vitro release of pDNA from the hydrogel scaffold occurred at 37 °C, in PBS at pH 7.4, with a sustained release of the gene without an initial burst. A total of 90% of pDNA is released in 5 days in the form of dendriplexes upon degradation of the hydrogel. Dendriplexes released from hydrogels successfully induced the expression of proteins in a 293T cell line and exhibited slightly lower transfection efficiency in cells than the freshly prepared pDNA dendriplexes (12 and 18% of transfected cells with dendriplexes released from hydrogels at 24 h and freshly prepared dendriplexes, respectively), due to their interaction with the hydrogel

scaffold. The NPs remained bioactive even after extended release (10% of transfected cells after 72 h release) and did not have any significant cytotoxic effect on the 293T cells, which demonstrated the utility of this approach for sustained gene delivery and further in vivo evaluation as gene delivery systems.

4. CONCLUSIONS AND FUTURE PERSPECTIVES

The unique nature of the dendritic architecture combined with its compositional preciseness affords hydrogels with tailored features and properties. Specifically, the defined composition, generation, molecular weight, viscosity, solubility, and end groups can be controlled. Moreover, hydrogel properties can be further tuned by selection of the linkage type contacting the macromonomers, be it covalent or physical interaction. Of particular interest are those hydrogels that are (1) physically cross-linked to yield materials that undergo self-repair or self-healing; (2) covalently cross-linked to afford stable or metastable materials that degrade on the time frame of the specific application; or (3) combined with other components (e.g., particles) to create composite materials to give unprecedented properties.

Consequently, dendritic hydrogels are being evaluated for a variety of biomedical and bioscience uses. For example, hydrogel sealants or scaffolds are reported for ocular, vascular, bone, and cartilage applications. However, significant opportunities still remain in this tissue repair space, as many of the above reports are a first in that area. Described below are four new potential areas where these hydrogels, applied as films, strips, pastes, spray, or as a liquid that transforms to a gel, may be of clinical utility and address a clear unmet clinical need.

- (1) Burns are one of the most common and devastating forms of trauma. Burn injuries (e.g., caused by fire, electricity, chemicals, radiation) are among the most challenging to manage: significant fluid loss and extensive tissue damage resulting from deep wounds impair multiple vital functions performed by skin. Wound infection, which further increases the local tissue damage, is a common complication, while systemic inflammatory and immunological responses lead to a higher predisposition to life-threatening sepsis and multiorgan failure. Early and appropriate clinical treatments are critical to reduce burn mortality rates. Thus, hydrogel wound dressings that provide transient physiologic wound closure, absorb wound exudate, prevent wound desiccation, isolate the wound from the environment, provide controlled delivery of antibiotic or anti-inflammatory agents, or can be easily changed and replaced in a pain-free manner are needed.
- (2) Spinal surgery exposes the spinal cord and its closely associated arterial and venous plexus to injury. Vascular bleeding is a primary concern as the postoperative risk of a cord hematoma has significant clinical consequence as potentially leading to cord compression and paralysis. Most surgical bleeding in spinal surgery is low pressure venous bleeding well suited to hemostasis with a hydrogel system. Additionally, cerebrospinal fluid leaks are common complications resulting, at best, in severe postoperative headaches or, at worse, in large collections that require further surgical draining leading to increased comorbidities. Hydrogels that can seal the site, preventing bleeding and cerebrospinal fluid leakage, are needed.

- (3) Surgery to highly perfused organs such as liver or spleen can result in large surfaces of active bleeding after trauma or during elective procedure. Transient control of bleeding with a hydrogel system may prove a very useful tool to limit intraoperative bleeding and reduce transfusion requirements and their complications. Thus, hydrogel sealants that assist the surgical procedure are needed.
- (4) Open-heart surgery such as valve replacements and some open vascular procedures can be complicated by leakage around valves or grafts postoperatively. As these patients require anticoagulation, the natural clotting cascade cannot be relied on to control this bleeding. There is, therefore, an opportunity to develop hydrogel-based hemostatic systems that better address this problem and enable closure of the wound site.

Reports on the use of dendritic hydrogels for drug (molecular, protein, nucleic acid) delivery are encouraging but limited in scope. Thus, there are significant opportunities, particularly for the delivery of small molecules (<1000 g/mol) and proteins. Controlling release rates of small molecules from hydrogels is challenging given that the pore size of the hydrogel is much larger than the size of the molecule. Taking advantage of the dendrimer core to sequester the agent in addition to the dendrimer being a structural unit for hydrogel formation is an elegant approach to this challenge. Given the number of protein therapeutics in use, and in development, there is a need for improved delivery via systemic and local approaches as well as control over the release rate, from days to months. As proteins are also easily denatured and lose their potency, this is an additional hurdle that must be overcome for protein delivery as it must be packaged and delivered via the hydrogel.

A renewed application area for dendritic hydrogels is as a synthetic extracellular matrix for controlling or directing cell fate. Applications can be envisioned that are clinical as well as in vitro. This represents a fertile area for additional study given the advances in stem cell biology and system biology, as the genetic reprogramming of cells is becoming routine. The use of small molecule based cocktails or genetic alterations are also likely to be enhanced by providing specific cues from the extracellular matrix or by providing a 3D environment for the cells to reside in where they encounter appropriate mechanical properties.⁷⁶ Dendrimer-based hydrogels may provide a means to such multifunctional hydrogels where the dendrimer is not only the structural unit for the hydrogel while providing specific mechanical and degradation properties, but also a site for linking specific chemical or biological cues.

As new research activities continue, it is also critical to transition these discoveries to development efforts and subsequent commercialization. The translation of a research idea to a commercial product is one measure of success, and represents an important milestone in this emerging area to encourage others to bring their ideas to the clinic. Dendritic polymers have not yet attained the widespread use as other polymer architectures, likely a consequence of cost and time associated with synthetic procedure, but advances in dendrimer synthesis are reducing this commercialization risk. Hyperbranch Medical Technology (HBMT) has commercialized the first dendritic hydrogel ocular sealant (OcuSeal) for the closure of wounds created by cataract, LASIK, corneal transplant procedures, as well as trauma. OcuSeal received CE Mark approval in 2007 and, in that same year, the first human

patients were treated. Building on that success, HBMT commercialized a hernia mesh sealant (Adherus Hernia Mesh Fixation, CE Mark 2009), a spinal sealant (Adherus Spinal Sealant, CE Mark 2009), and a dural sealant (Adherus Dural Sealant, CE Mark 2009 and FDA approval 2015).

In summary, significant accomplishments in dendritic based hydrogels are described in the literature over the past decade. These successes are a result of advances in the synthesis of dendrimers and dendritic polymers as well as in the fabrication methods to chemically or physically cross-link hydrogels. Subsequent evaluation of these hydrogels in a variety of clinically relevant *in vitro*, *ex vivo*, and *in vivo* models demonstrate the utility of these biomaterials. Work on dendritic polymers and hydrogels will continue to advance our understanding of the advantages and limitations of current materials, to spur critical discussions and analyses, as well as to afford new compositions and properties. We encourage others to explore this promising area at the intersection of materials and medicine, which has the potential to significantly impact society.

AUTHOR INFORMATION

Corresponding Author

*E-mail: mgrin@bu.edu.

Notes

The authors declare the following competing financial interest(s): MWG is a co-founder of Hyperbranch Medical Technology (HBMT).

ACKNOWLEDGMENTS

The authors thank Boston University National Institute of Health (R01EY13881 and R01EB021308) and Coulter Foundation for support. M.W.G. also thanks his past and current students and postdoctoral fellows, as well as our many clinical collaborators, for their hard work and dedication to synthesizing and evaluating new dendritic polymers and hydrogels.

REFERENCES

- (1) Wichterle, O.; Lim, D. *Nature* **1960**, *185*, 117–118.
- (2) Peppas, N. A.; Hilt, J. Z.; Khademhosseini, A.; Langer, R. *Adv. Mater.* **2006**, *18*, 1345–1360.
- (3) Hoffman, A. S. *Adv. Drug Delivery Rev.* **2002**, *54*, 3–12.
- (4) Du, X.; Zhou, J.; Shi, J.; Xu, B. *Chem. Rev.* **2015**, *115*, 13165–13307.
- (5) Zhang, H.; Grinstaff, M. W. *Macromol. Rapid Commun.* **2014**, *35*, 1906–1924.
- (6) Kopeček, J. J. *Polym. Sci., Part A: Polym. Chem.* **2009**, *47*, 5929–5946.
- (7) Vermonden, T.; Censi, R.; Hennink, W. E. *Chem. Rev.* **2012**, *112*, 2853–2888.
- (8) Yu, L.; Ding, J. *Chem. Soc. Rev.* **2008**, *37*, 1473–1481.
- (9) Ghobril, C.; Grinstaff, M. W. *Chem. Soc. Rev.* **2015**, *44*, 1820–1835.
- (10) Moon, H. J.; Ko, D. Y.; Park, M. H.; Joo, M. K.; Jeong, B. *Chem. Soc. Rev.* **2012**, *41*, 4860–4883.
- (11) Lee, K. Y.; Mooney, D. J. *Chem. Rev.* **2001**, *101*, 1869–1880.
- (12) Hu, B.-H.; Su, J.; Messersmith, P. B. *Biomacromolecules* **2009**, *10*, 2194–2200.
- (13) García, A. *Ann. Biomed. Eng.* **2014**, *42*, 312–322.
- (14) Nicodemus, G. D.; Bryant, S. J. *Tissue Eng., Part B* **2008**, *14*, 149–165.
- (15) Ifkovits, J. L.; Burdick, J. A. *Tissue Eng.* **2007**, *13*, 2369–2385.
- (16) Lapienis, G. *Prog. Polym. Sci.* **2009**, *34*, 852–892.
- (17) Bakaic, E.; Smeets, N. M. B.; Hoare, T. *RSC Adv.* **2015**, *5*, 35469–35486.
- (18) Gasteier, P.; Reska, A.; Schulte, P.; Salber, J.; Offenhäusser, A.; Moeller, M.; Groll, J. *Macromol. Biosci.* **2007**, *7*, 1010–1023.
- (19) Lin, C.-C. *RSC Adv.* **2015**, *5*, 39844–39853.
- (20) Oudshoorn, M. H. M.; Rissmann, R.; Bouwstra, J. A.; Hennink, W. E. *Biomaterials* **2006**, *27*, 5471–5479.
- (21) Zhang, H.; Bre, L.; Zhao, T.; Newland, B.; Da Costa, M.; Wang, W. J. *Mater. Chem. B* **2014**, *2*, 4067–4071.
- (22) Zhang, H.; Patel, A.; Gaharwar, A. K.; Mihaila, S. M.; Iviglia, G.; Mukundan, S.; Bae, H.; Yang, H.; Khademhosseini, A. *Biomacromolecules* **2013**, *14*, 1299–1310.
- (23) Liu, Y.; Zhang, F.; Ru, Y. *Carbohydr. Polym.* **2015**, *117*, 304–311.
- (24) Andrén, O. C. J.; Walter, M. V.; Yang, T.; Hult, A.; Malkoch, M. *Macromolecules* **2013**, *46*, 3726–3736.
- (25) Caminade, A.-M.; Yan, D.; Smith, D. K. *Chem. Soc. Rev.* **2015**, *44*, 3870–3873.
- (26) Grayson, S. M.; Fréchet, J. M. J. *Chem. Rev.* **2001**, *101*, 3819–3868.
- (27) Majoral, J.-P.; Caminade, A.-M. *Chem. Rev.* **1999**, *99*, 845–880.
- (28) Mintzer, M. A.; Grinstaff, M. W. *Chem. Soc. Rev.* **2011**, *40*, 173–190.
- (29) Newkome, G. R.; He, E.; Moorefield, C. N. *Chem. Rev.* **1999**, *99*, 1689–1746.
- (30) Esfand, R.; Tomalia, D. A. *Drug Discovery Today* **2001**, *6*, 427–436.
- (31) Smith, D. K. *Adv. Mater.* **2006**, *18*, 2773–2778.
- (32) Mongkhontreerat, S.; Andrén, O. C. J.; Boujemaoui, A.; Malkoch, M. J. *Polym. Sci., Part A: Polym. Chem.* **2015**, *53*, 2431–2439.
- (33) Newkome, G. R.; Baker, G. R.; Arai, S.; Saunders, M. J.; Russo, P. S.; Theriot, K. J.; Moorefield, C. N.; Rogers, L. E.; Miller, J. E. *J. Am. Chem. Soc.* **1990**, *112*, 8458–8465.
- (34) McWatt, M.; Boons, G.-J. *Eur. J. Org. Chem.* **2001**, *2001*, 2535–2545.
- (35) Marmillon, C.; Gauffre, F.; Gulik-Krzywicki, T.; Loup, C.; Caminade, A.-M.; Majoral, J.-P.; Vors, J.-P.; Rump, E. *Angew. Chem., Int. Ed.* **2001**, *40*, 2626–2629.
- (36) Gitsov, I.; Pracitto, R.; Lambrych, K. R. *Polym. Mater. Sci. Eng.* **1998**, *79*, 447–448.
- (37) Namazi, H.; Adeli, M. *Eur. Polym. J.* **2003**, *39*, 1491–1500.
- (38) Wu, X.-Y.; Huang, S.-W.; Zhang, J.-T.; Zhuo, R.-X. *Macromol. Biosci.* **2004**, *4*, 71–75.
- (39) Zhang, J.-T.; Huang, S.-W.; Zhuo, R.-X. *Macromol. Biosci.* **2004**, *4*, 575–578.
- (40) Wang, Q.; Mynar, J. L.; Yoshida, M.; Lee, E.; Lee, M.; Okuro, K.; Kinbara, K.; Aida, T. *Nature* **2010**, *463*, 339–343.
- (41) Huang, Z.; Lee, H.; Lee, E.; Kang, S.-K.; Nam, J.-M.; Lee, M. *Nat. Commun.* **2011**, *2*, 459.
- (42) Carnahan, M. A.; Middleton, C.; Kim, J.; Kim, T.; Grinstaff, M. W. *J. Am. Chem. Soc.* **2002**, *124*, 5291–5293.
- (43) Degoricija, L.; Bansal, P. N.; Söntjens, S. H. M.; Joshi, N. S.; Takahashi, M.; Snyder, B.; Grinstaff, M. W. *Biomacromolecules* **2008**, *9*, 2863–2872.
- (44) Wathier, M.; Jung, P. J.; Carnahan, M. A.; Kim, T.; Grinstaff, M. W. *J. Am. Chem. Soc.* **2004**, *126*, 12744–12745.
- (45) Wathier, M.; Johnson, M. S.; Carnahan, M. A.; Baer, C.; McCuen, B. W.; Kim, T.; Grinstaff, M. W. *ChemMedChem* **2006**, *1*, 821–825.
- (46) Oelker, A. M.; Berlin, J. A.; Wathier, M.; Grinstaff, M. W. *Biomacromolecules* **2011**, *12*, 1658–1665.
- (47) Ghobril, C.; Charoen, K.; Rodriguez, E. K.; Nazarian, A.; Grinstaff, M. W. *Angew. Chem., Int. Ed.* **2013**, *52*, 14070–14074.
- (48) Gitsov, I.; Zhu, C. *Macromolecules* **2002**, *35*, 8418–8427.
- (49) Zhu, C.; Hard, C.; Lin, C.; Gitsov, I. *J. Polym. Sci., Part A: Polym. Chem.* **2005**, *43*, 4017–4029.
- (50) Gitsov, I.; Zhu, C. *J. Am. Chem. Soc.* **2003**, *125*, 11228–11234.

- (51) Malkoch, M.; Vestberg, R.; Gupta, N.; Mespouille, L.; Dubois, P.; Mason, A. F.; Hedrick, J. L.; Liao, Q.; Frank, C. W.; Kingsbury, K.; Hawker, C. J. *Chem. Commun.* **2006**, 2774–2776.
- (52) Antoni, P.; Hed, Y.; Nordberg, A.; Nyström, D.; von Holst, H.; Hult, A.; Malkoch, M. *Angew. Chem., Int. Ed.* **2009**, *48*, 2126–2130.
- (53) Hed, Y.; Oberg, K.; Berg, S.; Nordberg, A.; von Holst, H.; Malkoch, M. *J. Mater. Chem. B* **2013**, *1*, 6015–6019.
- (54) Oberg, K.; Hed, Y.; Joelsson Rahmn, I.; Kelly, J.; Lowenhielm, P.; Malkoch, M. *Chem. Commun.* **2013**, *49*, 6938–6940.
- (55) Altin, H.; Kosif, I.; Sanyal, R. *Macromolecules* **2010**, *43*, 3801–3808.
- (56) Kaga, S.; Gevrek, T. N.; Sanyal, A.; Sanyal, R. *J. Polym. Sci., Part A: Polym. Chem.* **2016**, *54*, 926–934.
- (57) Grinstaff, M. W. *Biomaterials* **2007**, *28*, 5205–5214.
- (58) Oelker, A. M.; Grinstaff, M. W. *J. Mater. Chem.* **2008**, *18*, 2521–2536.
- (59) Luman, N. R.; Kim, T.; Grinstaff, M. W. *Pure Appl. Chem.* **2004**, *76*, 1375–1385.
- (60) Kang, P. C.; Carnahan, M. A.; Wathier, M.; Grinstaff, M. W.; Kim, T. *J. Cataract Refractive Surg.* **2005**, *31*, 1208–1212.
- (61) Degoricija, L.; Johnson, C. S.; Wathier, M.; Kim, T.; Grinstaff, M. W. *Invest. Ophthalmol. Visual Sci.* **2007**, *48*, 2037–2042.
- (62) Wathier, M.; Johnson, C. S.; Kim, T.; Grinstaff, M. W. *Bioconjugate Chem.* **2006**, *17*, 873–876.
- (63) Drury, J. L.; Mooney, D. J. *Biomaterials* **2003**, *24*, 4337–4351.
- (64) Söntjens, S. H. M.; Nettles, D. L.; Carnahan, M. A.; Setton, L. A.; Grinstaff, M. W. *Biomacromolecules* **2006**, *7*, 310–316.
- (65) Wang, Y.; Zhao, Q.; Zhang, H.; Yang, S.; Jia, X. *Adv. Mater.* **2014**, *26*, 4163–4167.
- (66) Navath, R. S.; Menjoge, A. R.; Dai, H.; Romero, R.; Kannan, S.; Kannan, R. M. *Mol. Pharmaceutics* **2011**, *8*, 1209–1223.
- (67) Holden, C. A.; Tyagi, P.; Thakur, A.; Kadam, R.; Jadhav, G.; Kompella, U. B.; Yang, H. *Nanomedicine* **2012**, *8*, 776–783.
- (68) Yang, H.; Tyagi, P.; Kadam, R. S.; Holden, C. A.; Kompella, U. B. *ACS Nano* **2012**, *6*, 7595–7606.
- (69) Parker, A. L.; Newman, C.; Briggs, S.; Seymour, L.; Sheridan, P. *J. Expert Rev. Mol. Med.* **2003**, *5*, 1–15.
- (70) Mintzer, M. A.; Simanek, E. E. *Chem. Rev.* **2009**, *109*, 259–302.
- (71) Love, K. T.; Mahon, K. P.; Levins, C. G.; Whitehead, K. A.; Querbes, W.; Dorkin, J. R.; Qin, J.; Cantley, W.; Qin, L. L.; Racie, T.; Frank-Kamenetsky, M.; Yip, K. N.; Alvarez, R.; Sah, D. W. Y.; de Fogerolles, A.; Fitzgerald, K.; Kotliansky, V.; Akinc, A.; Langer, R.; Anderson, D. G. *Proc. Natl. Acad. Sci. U. S. A.* **2010**, *107*, 1864–1869.
- (72) Akinc, A.; Goldberg, M.; Qin, J.; Dorkin, J. R.; Gamba-Vitalo, C.; Maier, M.; Jayaprakash, K. N.; Jayaraman, M.; Rajeev, K. G.; Manoharan, M.; Kotliansky, V.; Rohl, I.; Leshchiner, E. S.; Langer, R.; Anderson, D. G. *Mol. Ther.* **2009**, *17*, 872–879.
- (73) Akinc, A.; Zumbuehl, A.; Goldberg, M.; Leshchiner, E. S.; Busini, V.; Hossain, N.; Bacallado, S. A.; Nguyen, D. N.; Fuller, J.; Alvarez, R.; Borodovsky, A.; Borland, T.; Constien, R.; de Fogerolles, A.; Dorkin, J. R.; Narayanannair Jayaprakash, K.; Jayaraman, M.; John, M.; Kotliansky, V.; Manoharan, M.; Nechev, L.; Qin, J.; Racie, T.; Raitcheva, D.; Rajeev, K. G.; Sah, D. W. Y.; Soutschek, J.; Toudjarska, I.; Vornlocher, H.-P.; Zimmermann, T. S.; Langer, R.; Anderson, D. G. *Nat. Biotechnol.* **2008**, *26*, 561–569.
- (74) Dufès, C.; Uchegbu, I. F.; Schätzlein, A. G. *Adv. Drug Delivery Rev.* **2005**, *57*, 2177–2202.
- (75) Deng, J.; Luo, Y.; Zhang, L.-M. *Soft Matter* **2011**, *7*, 5944–5947.
- (76) Charoen, K. M.; Fallica, B.; Colson, Y. L.; Zaman, M. H.; Grinstaff, M. W. *Biomaterials* **2014**, *35*, 2264–2271.
- (77) Nordberg, A.; Antoni, P.; Montanez, M. I.; Hult, A.; Von Holst, H.; Malkoch, M. *ACS Appl. Mater. Interfaces* **2010**, *2*, 654–657.